Title

Synthetic peripherally-restricted cannabinoid suppresses chemotherapy-induced peripheral neuropathy pain symptoms by CB1 receptor activation.

Authors

Mulpuri, Yatendra
Marty, Vincent N
Munier, Joseph J
et al.

Publication Date

2018-09-01

DOI

10.1016/j.neuropharm.2018.07.002

Peer reviewed

Journal of Medicinal Chemistry

Article

pubs.acs.org/jmc

Peripherally Selective Cannabinoid 1 Receptor (CB1R) Agonists for the Treatment of Neuropathic Pain

Herbert H. Seltzman,*[,†] Craig Shiner,[†] Erin E. Hirt,[†] Anne F. Gilliam,[†] Brian F. Thomas,[†] Rangan Maitra,[†] Rod Snyder,[†] Sherry L. Black,[†] Purvi R. Patel,[†] Yatendra Mulpuri,[‡] and Igor Spigelman*[,‡]

[†]Center for Drug Discovery, Research Triangle Institute, Research Triangle Park, North Carolina 27709, United States

[‡]Division of Oral Biology & Medicine, School of Dentistry, University of California, 10833 Le Conte Avenue, 63-078 CHS, Los Angeles, California 090095-1668, United States

Supporting Information

ABSTRACT: Alleviation of neuropathic pain by cannabinoids is limited by their central nervous system (CNS) side effects. Indole and indene compounds were engineered for high hCB1R affinity, peripheral selectivity, metabolic stability, and in vivo efficacy. An epithelial cell line assay identified candidates with <1% blood−brain barrier penetration for testing in a rat neuropathy induced by unilateral sciatic nerve entrapment (SNE). The SNE-induced mechanical allodynia was reversibly suppressed, partially or completely, after intraperitoneal or oral administration of several indenes. At doses that relieve neuropathy symptoms, the indenes completely lacked, while the brain-permeant CB1R agonist HU-210 (**1**) exhibited strong CNS side effects, in catalepsy, hypothermia, and motor incoordination assays. Pharmacokinetic findings of ∼0.001 cerebrospinal fluid:plasma ratio further supported limited CNS penetration. Pretreatment with selective CB1R or CB2R blockers suggested mainly CB1R contribution to an indene's antiallodynic effects. Therefore, this class of CB1R agonists holds promise as a viable treatment for neuropathic pain.

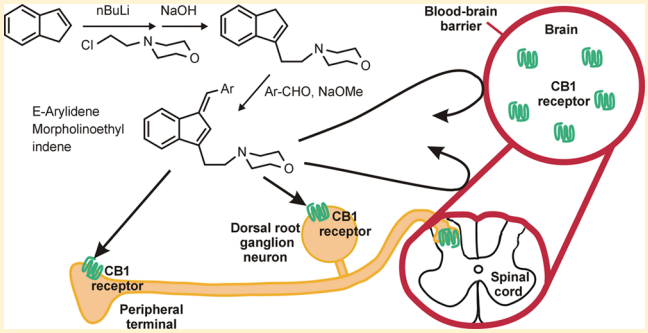

INTRODUCTION

Various neuropathies and chronic inflammatory conditions pose a major socioeconomic and clinical challenge[1] in part because of poorly understood etiologies and mechanisms and in part because side effects of existing treatments greatly limit their effectiveness.[2] This includes synthetic and naturally occurring cannabinoids (CBs), which reduce the hyperalgesia and allodynia associated with persistent pain of neuropathic and inflammatory origin in humans[3] and animals[4] yet they exhibit side effects mediated primarily by activation of central nervous system (CNS) CB1 receptors (CB1Rs). These psychotropic CNS effects also account for the abuse potential of plant-based and synthetic CBs.

In addition to their CNS expression, CB1Rs, CB2Rs, and their endogenous ligands (endocannabinoids, ECBs) have a diverse distribution in peripheral tissues, including primary afferent neurons.[5] Local administration of CBs into inflamed tissue attenuates hyperalgesia and allodynia via peripheral CBRs at doses that produce minimal CNS-mediated side effects.[6] The crucial role of peripheral CBRs in the antihyperalgesic actions of systemically administered CBs was demonstrated using conditional deletion of CB1Rs located on nociceptive primary afferent neurons.[7] Also, many studies have demonstrated increases in expression of CB1Rs, CB2Rs, and ECBs, both in the peripheral tissues and the CNS, during inflammation and after development of painful neuropathies, reviewed in ref 8. Increases in CBR expression result in increased potency or efficacy of the exogenously applied CBs[9] and may also account for the effectiveness of CBs in alleviating neuropathic pain symptoms after chronic repeated treatment,[10] unlike opioids, which have only limited long-term effectiveness.[11] While selective activation of CB2Rs also inhibits experimentally induced inflammatory pain and itch or the persistent pain of neuropathic origin,[10b,12] activation of both CB1R and CB2Rs appears to have synergistic effects on pain suppression.[12a] These studies provided a rationale for the development of peripherally acting endocannabinoid-based therapeutic interventions.[13]

With the aim of utilizing the demonstrated benefits of CBs to sustainably ameliorate neuropathic pain, we sought to develop peripherally restricted CB1R agonists, which would not penetrate the blood−brain barrier (BBB) so as to avoid the unwanted psychomimetic effects such as those caused by Δ^9-tetrahydrocannabinol (Δ^9-THC) that are also associated with activation of central CB1Rs. Peripheral restriction can be addressed by (1) the inclusion of charge that typically prevents BBB penetration in the absence of active transport, (2) the presence of actively effluxed moieties such as carboxylates, and (3) adjustment of partition coefficient and the topological polar surface area. Other factors potentially impact peripheral

Received: April 15, 2016
Published: August 2, 2016

DOI: 10.1021/acs.jmedchem.6b00516
J. Med. Chem. 2016, 59, 7525−7543

Scheme 1

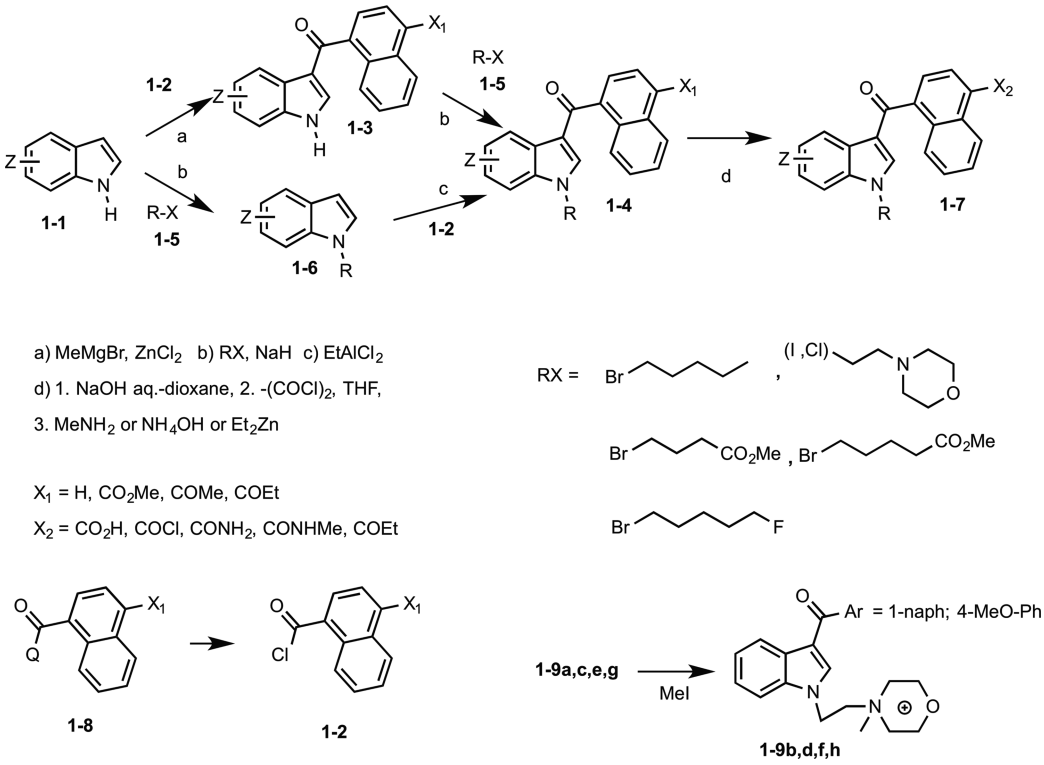

restriction such as activation of CB2Rs on the BBB endothelial cells.[14] We chose to examine indoles and indenes that have been demonstrated as ligands for CB1R agonist activity as starting points for modifications toward these ends.

RESULTS

Synthesis of Indoles. The synthesis of the target indoles where the 4-substituent of the naphthyl ring was alkyl or hydrogen followed the established general approaches shown in Scheme 1.[15] The synthesis of indoles with a 4-acyl substituted naphthylene ring required further modifications as described below. The acylation of indole **1-1** with the naphthoyl chloride **1-2a** (X_1 = CO_2Me) mediated by methyl magnesium bromide and zinc chloride afforded the corresponding **1-3b** in greater than 80% yield on scales of 20 g. Subsequent alkylation of **1-3b** with *n*-pentyl bromide proceeded in yields of about 50% of **1-4a** (X_1 = CO_2Me) on a 1 g scale. Upon scale up to 10 and 15 g, the alkylation step did not proceed to completion. Further, work up resulted in hydroxysis or transesterification to the *N*-alkylated or unalkylated acid or ethyl ester (when ethyl acetate was employed in the work up) that can likely be addressed with modified work up conditions.

Conversion of **1-4a** to other 4-substituted naphthoyl indoles was achieved by saponification to the acid **1-7a** (X_2 = CO_2H, R = Pn), which was converted to the acid chloride (X_2 = COCl, R = Pn) with oxalyl chloride and subsequently to the secondary amide **1-7b** (X_2 = CONHMe, R = Pn) (87%) with methylamine and to the primary amide **1-7c** (X_2 = $CONH_2$) (98%) with ammonium hydroxide. Conversion of the acid chloride to the methyl or ethyl ketones **1-7e,d** (X_2 = COMe, COEt) by treatment with either methyl Grignard (no product), dimethyl zinc (trace product), diethyl zinc (trace product), or triethyl aluminum (no product) was disappointing.

An alternative sequence to **1-7e,d** of first preparing the 4-substituted 1-naphthoyl chloride **1-2c,d** (X_1 = COMe, COEt) followed by coupling to the indole (*N*-alkylated or not) was examined in an effort to improve yields. Thus, commercially available 4-(methoxycarbonyl)naphthalene-1-carboxylic acid (**1-8a**) was converted to **1-2a** (X_1 = CO_2Me), then treated with dimethyl or diethyl zinc to afford **1-8b,c** (X_1 = COEt, COMe) in 63% and 37%, respectively, followed by hydrolysis of the esters to the acids **1-8d,e** in greater than 90% yield and treatment with oxalyl chloride to afford **1-2c,d** in near quantitative yield. Acylating indole **1-1** with **1-2d** (X_1 = COEt) mediated with MeMgBr afforded a 55% yield of **1-3d** (X_1 = COEt). Alkylation of **1-3d** with *n*-pentyl bromide, however, afforded no target compound (the product obtained from the low yield diethyl zinc reaction above was used for testing). Attempting synthesis of the methyl ketone analogue **1-7e** (X_2 = COMe) by reversing the sequence to acylating the prealkylated **1-6a** (R = Pn) with **1-2c** (X_1 = COMe) mediated by ethylaluminum dichloride gave a complex mixture with minimal **1−7e** (X_2 = COMe) that could not be isolated in pure form.

N-*ω*-Carboxyalkyl-indoles (butanoates and pentanoates, **1-4f** and **1-4g**, respectively) were prepared by acylation of indole **1-1a** with **1-2e** mediated by methylmagnesium bromide affording the naphthoylindole **1-3a**, which was then alkylated with ethyl *ω*-bromoalkanoate and sodium hydride to yield the corresponding ethyl butanoate and pentanoate and followed by hydrolysis to provide the corresponding acids **1-4f,g** (R = $-(CH_2)_n$-CO_2H, *n* = 3,4).[16]

Fluoroindole analogues were prepared from commercially available fluoroindole substituted in the 4, 5, 6, or 7-position (**1-1b−e**, Z = F) via acylation with **1-2e** (X_1 = H) in the presence of MeMgBr and $ZnCl_2$ to afford **1-3e−h** in 70−85% yields followed by alkylation with *n*-pentyl bromide/NaH to give **1-4h−k** (Z = F) in >80% yields. The 4-fluoro indole **1-3e** was also alkylated

DOI: 10.1021/acs.jmedchem.6b00516
J. Med. Chem. 2016, 59, 7525−7543

Scheme 2

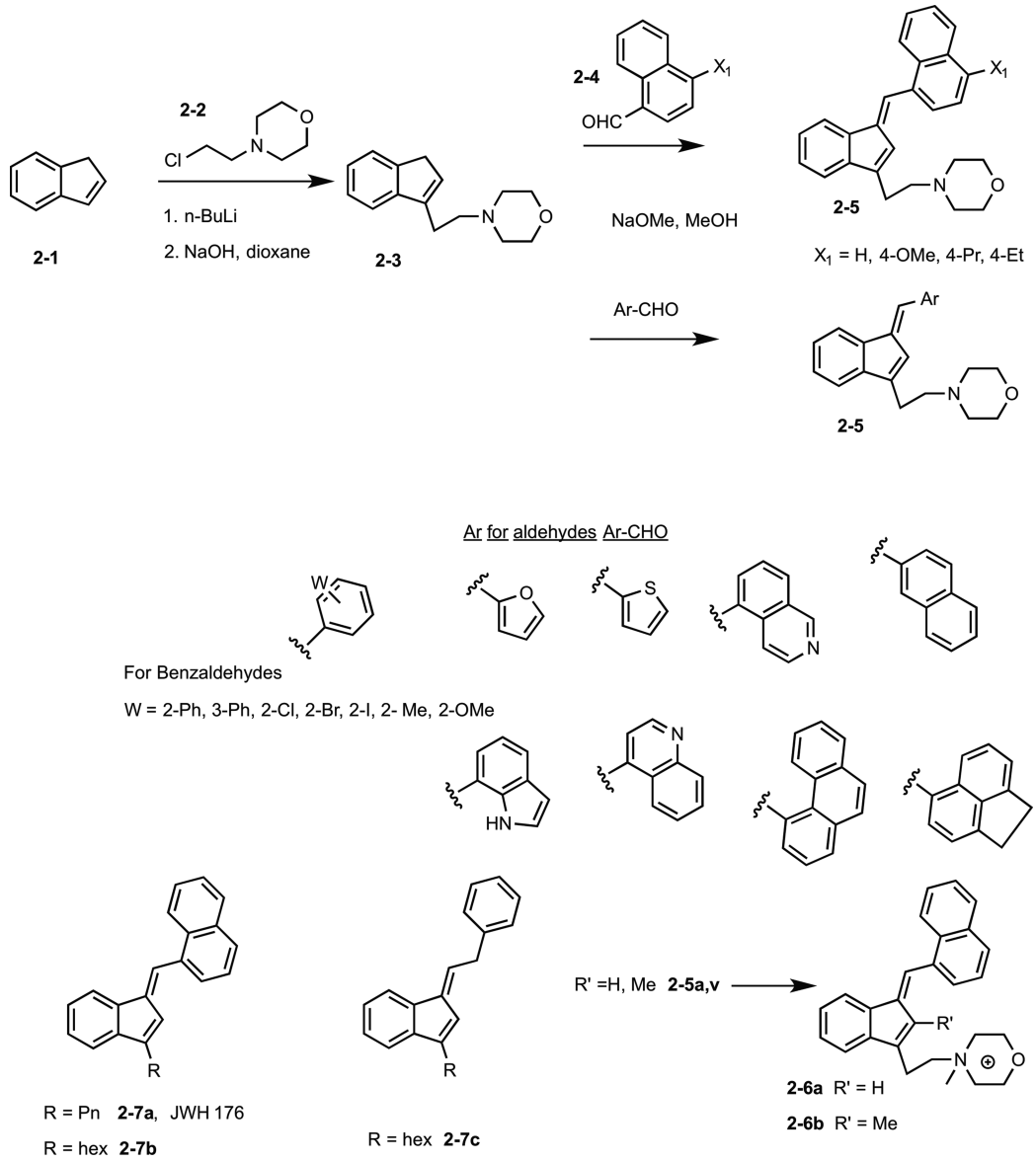

with 5-fluoro-1-bromopentane/NaH to give the corresponding **1-4l** in 27% yield. Similar alkylation with iodoethylmorpholine/NaH afforded **1-4m** (X_1 = H, Z = 4-F, R = morpholinoethyl) in 68% yield after chloroethylmorpholine did not alkylate **1-3e** (Z = 4-F). The analogue **1-4n** (X_1 = *n*-propyl, Z = 4-F, R = 5-F-pentyl) was prepared from 4-fluoroindole **1-1b** by acylation with 4-*n*-propyl-1-naphthoyl chloride (**1-2b**, X_1 = *n*-propyl) (MeMgBr, $ZnCl_2$) (58%), followed by alkylation with 5-fluoro-1-bromopentane/NaH to give the corresponding **1-4n** in 24% yield.

Synthesis of Indenes. Synthesis of the target 4-substituted naphthylidene- or substituted benzylidene-3-morpholinoethyl-2-indenes (**2-5**) with the *E*-olefin geometry was achieved as shown in Scheme 2 by alkylation of lithiated indene **2-1** with 1-chloro-2-(4-morpholino)ethane (**2-2**) to afford a mixture of the 1- and 3-alkylated 1*H*-indenes. Treatment of the mixture with sodium hydroxide induced isomerization to the more stable 3-(4-morpholinoethane)-1*H*-indene[17] (**2-3**) in 45% yield (Z = H). Treatment of **2-3** with the appropriate 1-naphthaldehyde, benzaldehyde, or aryl aldehyde in the presence of sodium methoxide gave the target *E*-olefin **2-5a–s** after either 18 h of heating at reflux (in 66% yield **2-5a**) or microwave heating. Microwave heating provided the same product more expeditiously in 15 min at 105 °C but in lesser yield (53% **2-5a**), a process that we employed for the majority of the analogues which were obtained in >90% purity (HPLC). Phenyl acetaldehyde, 4-hydroxy-1-naphthaldehyde, 2-nitro-, and 2-cyano-benzaldehyde were not ammenable to this method of synthesis, but particular interest in preparing and testing the phenyl acetaldehyde derived product, (1*E*)-3-hexyl-1-(2-phenylethylidene)-1*H*-indene (**2-7**) with only a distal aromatic ring (see above), was achieved by Horner–Wittig chemistry.[17] The *E*-geometry was established for the **2-5a–s** analogues by comparison of the ^{1}H NMR on the architype *E*-(1-naphthylidene)-3-morpholinoethyl-2-indenes prepared via the condensation chemistry from **2-3** with that prepared by Horner–Wittig chemistry that was characterized by NOE NMR spectroscopy.[17]

Neuropathy Testing. We examined the effectiveness of select indenes in alleviating the painful symptoms of neuropathy induced by unilateral sciatic nerve entrapment (SNE).[18] SNE was demonstrated to produce consistent pain behaviors,[18,19] a

DOI: 10.1021/acs.jmedchem.6b00516
J. Med. Chem. 2016, 59, 7525–7543

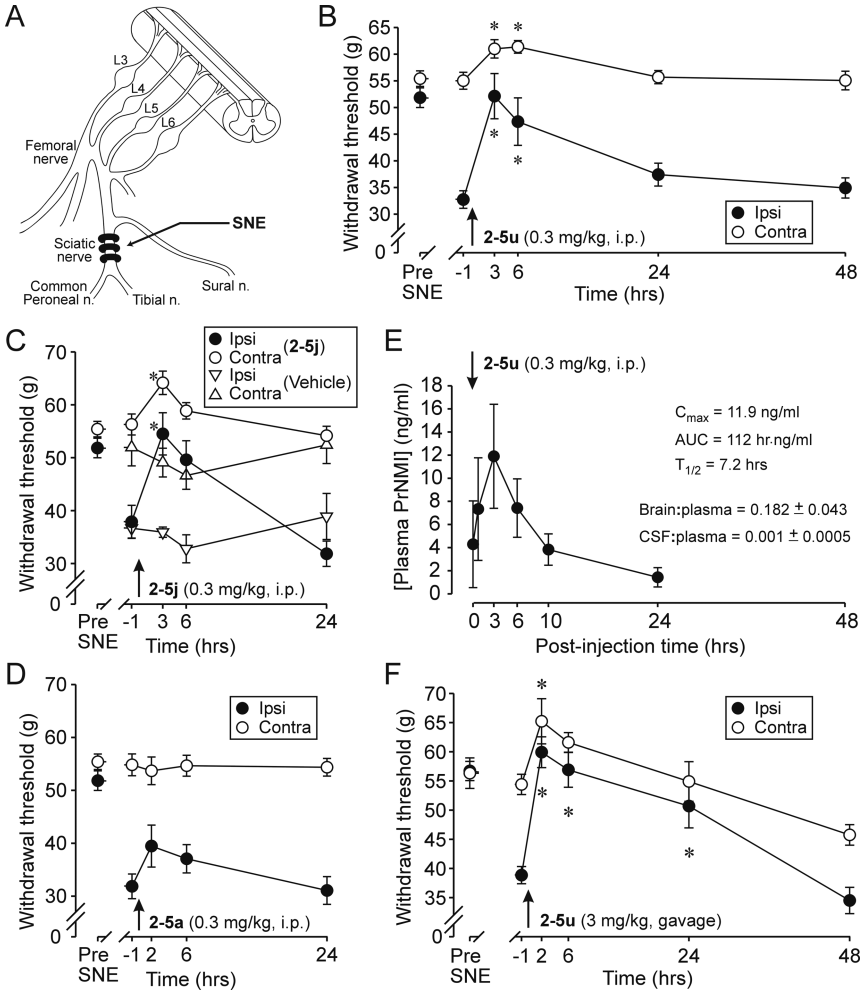

Figure 1. Reversible suppression of SNE-induced mechanical allodynia by representative indenes. (A) Schematic of sciatic nerve entrapment and relevant peripheral nerve and spinal ganglia. (B) Graph of withdrawal thresholds to mechanical stimulation of hindpaws ipsilateral and contralateral to SNE at 1 h before and 3, 6, 24, and 48 h after **2-5u** (0.3 mg/kg, ip) injection. At 3 h postinjection, ipsilateral thresholds are increased to levels of predrug contralateral thresholds and are indistinguishable from thresholds measured prior to neuropathy development (pre-SNE). Also note the drug-induced small, but significant increases in contralateral thresholds (mean ± SEM, $n = 8$ rats). (C) In the same rats, administration of **2-5j** (0.3 mg/kg), but not vehicle alone, results in similar increases in ipsilateral thresholds to pre-SNE values. (D) **2-5a** (0.3 mg/kg) produces considerably smaller increases in thresholds than **2-5u** or **2-5j**. (E) Changes in plasma [**2-5u**] and calculated pharmacokinetic parameters after injection (0.3 mg/kg, ip) in naïve rats ($n = 3$) are consistent with the time course of its effects on SNE neuropathy symptoms. Brain and CSF/plasma ratios of PrNMI obtained from samples collected from 3 other rats at ∼75 min after **2-5u** (0.3 mg/kg, ip) suggest minimal CNS penetration. (F) Oral administration of **2-5u** (3 mg/kg) reversibly suppresses SNE neuropathy symptoms ($n = 8$ rats). *, $p < 0.05$ vs predrug (−1 h) values (one-way RM ANOVA).

transient loss of varicosities in nociceptive fibers,[20] and increased excitability of sciatic nerve.[21] The hyperexcitability and ectopic burst discharge of primary sensory neurons are widely considered as major contributors to pain symptomatology of peripheral neuropathy models. The SNE-induced mechanical allodynia models the most common complaint of human neuropathy patients of dynamic mechanical allodynia. Figure 1 illustrates that systemic injection of 0.3 mg/kg of PrNMI (**2-5u**) or MoNMI (**2-5j**) results in large, reversible decreases in mechanical allodynia. By contrast, ENMI (**2-5a**) has a much smaller effect, consistent with its lower CBR affinity and faster metabolism (Table 2).

Pharmacokinetics. Analysis of plasma samples after **2-5u** injections yielded its initial pharmacokinetic profile (Figure 1E), which was in good agreement with its antiallodynic effects (Figure 1B). Measurements of drug brain penetration include drug partitioned into brain lipids + unbound drug in equilibrium with extracellular fluid. The cerebrospinal fluid (CSF)/plasma ratios are considered to be more precise estimates of a drug's brain penetration because of the continuity of CSF with extracellular space.[22] However, both measures are needed to confirm minimal CNS access and to compare with other reported peripherally restricted CB1R ligands.[13c,23] Analysis of plasma, brain, and CSF samples confirmed the minimal penetration of **2-5u** into the CNS after systemic administration (Figure 1E).

In subsequent experiments, we demonstrated that **2-5u** was also effective in suppressing neuropathy symptoms after oral administration, which is more representative of future therapeutic uses. The high oral dose of **2-5u** (3 mg/kg) likely accounts for its continued antiallodynic effectiveness at the 24 h time point (Figure 1F).

Tetrad Testing. The CNS-mediated psychotropic actions of CB1R ligands represent their most troubling side effects. The catalepsy, motor performance, hypothermia, and analgesia tests are classically predictive of CNS CB1R activation.[24] Effects in all

DOI: 10.1021/acs.jmedchem.6b00516
J. Med. Chem. 2016, 59, 7525−7543

Scheme 3

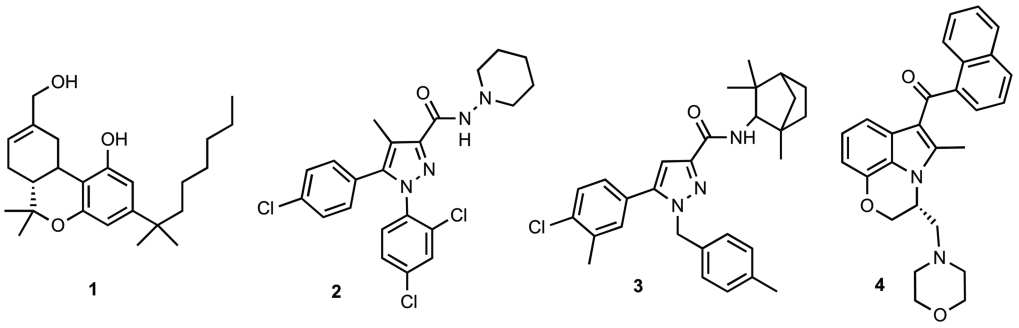

four tests have been thought to be mediated by the activation of central CB1Rs, but it is now well established that peripheral CBRs make a major contribution to the analgesic effects of CBs.[6d,12a,c] We used the "tetrad" to determine whether the novel ligands have antinociceptive effects and side effect profile consistent with central CB1R activation. We also studied the potent CB1R agonist, **1** (HU-210, Scheme 3)[25] (Tocris Bioscience, Ellisville, MO), to allow comparisons of this positive control with the putatively brain-impermeant analogues. The systemic doses of **1**[4b] and of novel indenes (e.g., Figure 1) were consistent with their demonstrated effectiveness in alleviating painful neuropathy symptoms. The "tetrad" tests were modified for rats, with rotarod substituting for the spontaneous activity test. Unlike **1**, **2-5u** and other indenes lack effects in the catalepsy, rotarod, or hypothermia assays, although a small effect in the tail-flick assay is observed, as expected for analgesic peripherally acting CB1R ligands (Figure 2).

CB1Rs Mediate Antiallodynic Effects of 2-5u. Despite similar affinities for the CB1R and CB2R subtypes, indene PRCBs are full agonists at hCB1R but only partial agonists at hCB2R (Table 2). To determine which receptor subtype is responsible for the antiallodynic effects of the novel CBR ligands in the SNE neuropathy, we measured the ability of a representative ligand, **2-5u**, to suppress mechanical allodynia in SNE rats in the presence of either CB1R or CB2R selective antagonists. **2-5u** was administered alone or 30 min after pretreatment with CBR blockers in SNE rats at 3-day intervals (Figure 3A). Pretreatment with the CB1R inverse agonist, SR141716 (**2**, Scheme 3),[26] completely blocked the antiallodynic effect of **2-5u** (Figure 3B,E), whereas pretreatment with a CB2R selective inverse agonist, SR144528 (**3**, Scheme 3), had little effect on suppression of allodynia by **2-5u** (Figure 3D). In the same rats, pretreatment with a peripherally restricted analogue of **2**, **18A**, recently developed by our group,[27] also prevented the antiallodynic effect of **2-5u** (Figure 3C,E). These studies demonstrated the CB1R dependence of **2-5u**'s antiallodynic effects in the SNE neuropathy.

DISCUSSION

Structure–Activity Relationships (SAR). The introduction of charge to CB1R ligands to impart peripheral selectivity was explored via quaternization of morpholinoethyl-indoles and -indenes of demonstrated CB1R agonists. Thus, morpholinoethylindoles 1-[2-(4-morpholino)ethyl]-3-(1-naphthoyl)indole (**1-9a**, JWH-200),[15a] 1-[2-(4-morpholino)ethyl]-3-(4-methoxy-1-naphthoyl)indole (**1-9c**, JWH-198),[15a] and 1-[2-(4-morpholino)ethyl]-3-(4-methyl-1-naphthoyl)indole (**1-9e**, JWH-193),[15a] respectively, and pravadoline[28] **1-9g** were quaternized to **1-9b,d,f,h**. Also, conformationally constrained morpholinoethyl indenes, (**2-5a**, *E*-4-[2-[1-(1-naphthalenylmethylene)-1*H*-inden-3-yl]ethyl]morpholine)[17] and its 2-methyl analogue **2-5v**, were quaternized to afford the corresponding charged quaternary ammonium analogues (**2-6a** and **2-6b**). Both of these changes resulted in a reduction of hCB1R binding affinity of between one and 2 orders of magnitude (see Table 1). Similarly, alkyl carboxy chains linked to the indole nitrogen as *ω*-butanoic (**1-4f**) and -pentanoic (**1-4g**) acids, as putative effluxed moieties, also exhibited no hCB1R affinity (K_i = > 10 μM) in contrast to the unmodified pentyl chain of 3-(naphthalene-1-carbonyl)-1-pentyl-1*H*-indole, JWH-018 (**1-4p**) (K_i = 4.3 nM).[15a] The 4-carboxy substituted naphthoyl analogue **1-7a** also showed no receptor affinity (K_i = >10 μM). These results steered our efforts away from charged analogues.

Screening results of peripheral selectivity and hCB1R affinity on our early analogues redirected ligand design. The peripheral selectivity of the high affinity compounds was tested in the Madin–Darby canine kidney (MDCK) epithelial cell line assay as a model of the BBB[29] and showed an association with the *n*-pentyl indoles and morpholinoethyl indenes, respectively. Thus, the *N*-pentyl 4-carboxy methyl ester indole **1-4a** was compared to the *N*-morpholinoethyl 4-carboxy methyl ester indole analogue **1-4o**. The basolateral:apical ratio (B:A) of the *n*-pentyl analogue **1-4a** was 0.00, while that of the *N*-morpholinoethyl analogue **1-4o** was 1.02, indicating nonpermeability of **1-4a** and equal central:peripheral distribution of **1-4o** in the MDCK model. This would suggest similar permeability for these indole analogues across the BBB.

The morpholinoethyl indene **2-5a**[17] and the *n*-pentyl indene 1-{[(1*E*)-3-pentyl-1*H*-inden-1-ylidene]methyl}naphthalene, JWH-176,[15a] **2-7a**, were also chosen as candidates for modification as they had high affinity for the CB1R (K_i = 4.69 and 17.2 nM, respectively). Surprisingly, both tested in the MDCK assay[29] as peripherally restricted (B:A = 0.00 and 0.04, respectively) with the morpholinoethyl moiety **2-5a**, showing slightly greater preferral restriction over the pentyl moiety (**2-7a**). This is the opposite order of the indole morpholinoethyl and the indole pentyl side chain pair tested (above) and of significant difference of B:A of the morpholinoethyl substituted indole **1-4o**. Thus, subsequent indene modifications were evolved from the morpholinoethyl indene analogue **2-5a** and subsequent indole modifications were evolved from *n*-pentyl indoles to examine SAR trends in affinity, MDCK permeability, and metabolic stability in order to select candidates for in vivo testing.

The effect upon hCB1R affinity of substituting the naphthoyl 4-position on the indoles, which has been associated with high receptor affinity in reported analogues,[15b] was examined in the *N*-pentyl family. Thus, in contrast to the 4-carboxy substituted naphthoyl analogue **1-7a** (K_i = >10 μM), the corresponding ethyl

DOI: 10.1021/acs.jmedchem.6b00516
J. Med. Chem. 2016, 59, 7525–7543

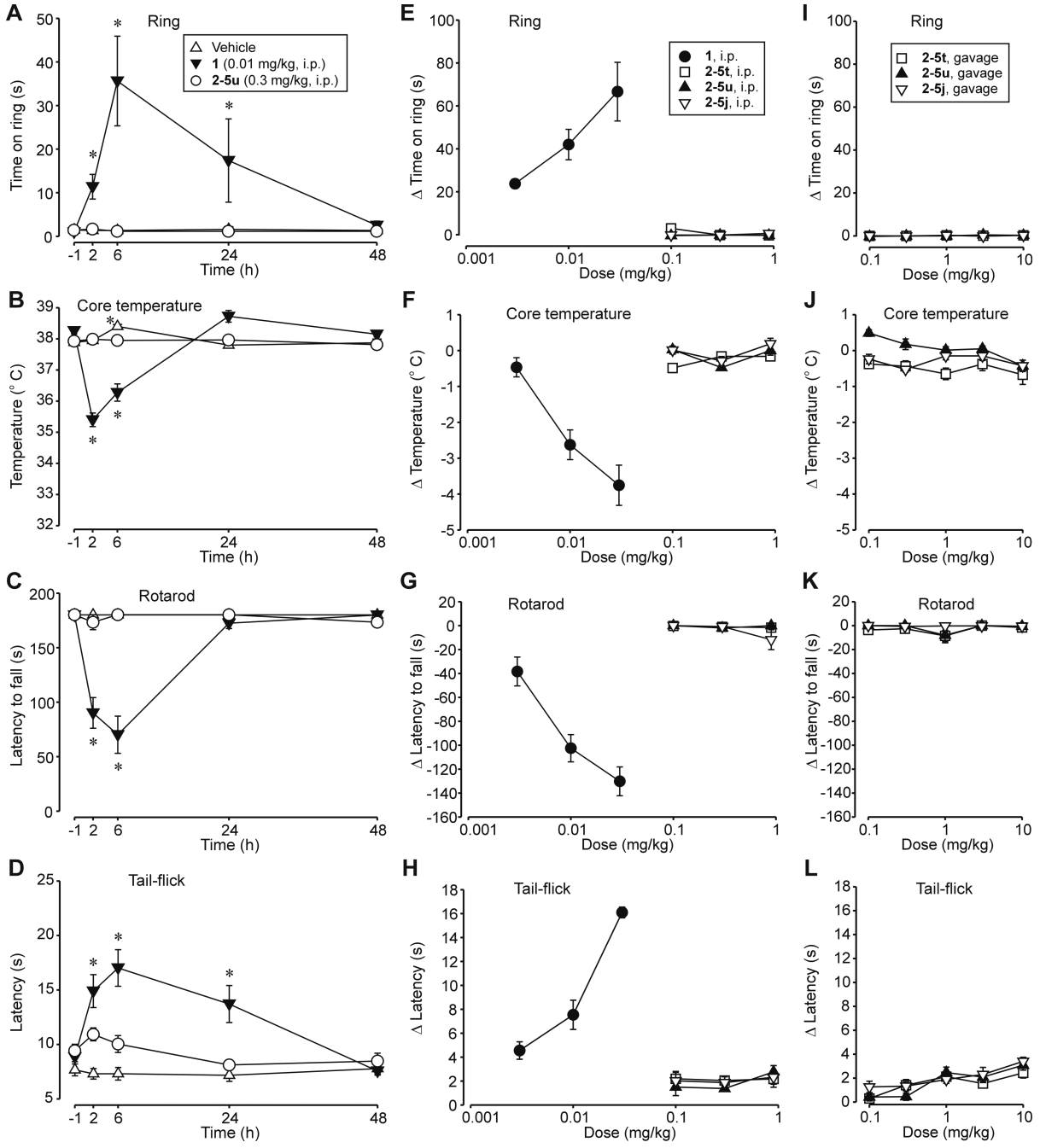

Figure 2. Activity of **1**, **2-5u**, **2-5t**, and **2-5j** in the "tetrad" assays. (A–D) Rats were tested in each assay 1 h prior and up to 48 h following intraperitoneal injection of vehicle, **1** (0.01 mg/kg) or **2-5u** (0.3 mg/kg). Note the profound CNS side effects of **1** vs **2-5u** in the ring, core temperature, and rotarod tests. The small analgesic effect of **2-5u** in the tail-flick assay is consistent with peripheral activation of CBRs. *, $p < 0.05$ vs predrug (−1 h) values (one-way RM ANOVA). (E–H) Dose-dependence of brain-permeant **1** and compounds **2-5t**, **2-5u**, or **2-5j** in the tetrad assays after intraperitoneal administration. Each point represents mean peak effect ± SEM of **1** ($n = 6$ rats), **2-5t** ($n = 8$ rats), **2-5u** ($n = 8$ rats), and **2-5j** ($n = 8$ rats), each subtracted from its vehicle control. (I–L) Dose-dependence of **2-5t**, **2-5u**, and **2-5j** in the tetrad assays after oral administration. Each point represents mean peak effect ± SEM of **2-5t** ($n = 8$ rats), **2-5u** ($n = 8$ rats), and **2-5j** ($n = 8$ rats), each subtracted from its vehicle control. Note the relative lack of side effects in the catalepsy, motor incoordination, and hypothermia assays. The small effects in the tail-flick assay are consistent with antinociceptive effects due to activation of peripheral CBRs in naïve rats.

ester (**1-4c**) exhibited a $K_i = 115$ nM and the shorter methyl ester (**1-4a**) exhibited a $K_i = 20$ nM. The three atom-long chain 4-propanoyl-naphthyl analogue (**1-7d**) exhibited a $K_i = 5.7$ nM. The 4-*N*-methylamido analogue **1-7b** ($K_i = 127$ nM) was less active than its isosteric oxygen or carbon analogues (**1-4a** and **1-7d**). The 4-amido analogue (**1-7c**), however, had higher affinity for hCB1R ($K_i = 96$ nM) than the corresponding acid **1-7a**.

A similar effect of the 4-position substituent was observed for the indenes in the morpholinoethyl family. The hCB1R affinity progressed from 4-H (4.69 nM) (**2-5a**) to 4-OMe (2.43 nM) (**2-5j**) to 4-*n*-Pr (1.18 nM) (**2-5u**) to 4-Et (0.86 nM) (**2-5t**), all of which were subsequently tested in vivo.

Modeling and SAR studies of indole CB1R agonists and, similarly for the indene mimics of the indoles, support that the

DOI: 10.1021/acs.jmedchem.6b00516
J. Med. Chem. 2016, 59, 7525–7543

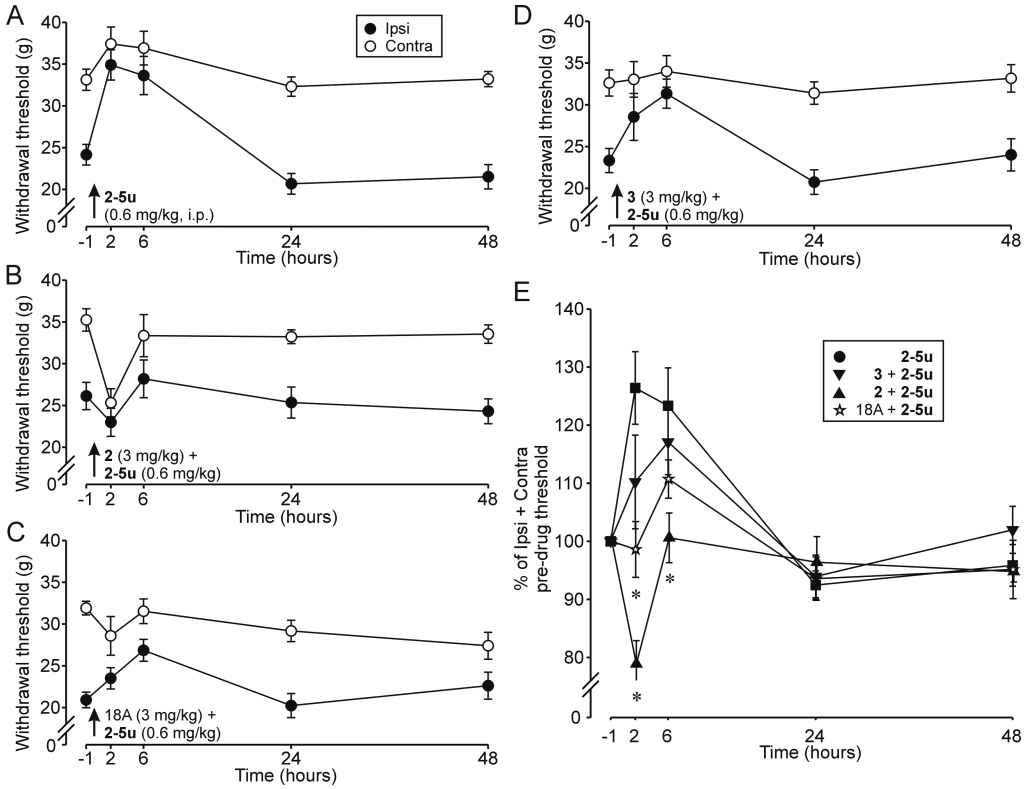

Figure 3. CB1Rs mediate antiallodynic effects of **2-5u** in the SNE neuropathy. (A) Suppression of SNE-induced mechanical allodynia by **2-5u** (0.6 mg/kg). (B) In the same rats (n = 8), pretreatment with the CB1R inhibitor **2** (rimonabant, 3 mg/kg, ip) completely blocks the response to **2-5u**. (C) A peripherally restricted rimonabant analogue, **18A**, also blocked the response to **2-5u**. (D) By contrast, the selective CB2R inhibitor **3** (3 mg/kg, ip) produced only a small decrease in the response to **2-5u**. (E) Summary of effects of selective CB1R and CB2R inhibition on antiallodynic effects of **2-5u**. *, $p < 0.05$ vs treatment with **2-5u** alone (one-way ANOVA).

favored conformation of the naphthoyl ring for binding/activation in the analogues of **1-4p** and **5** (WIN 55,212-2)[28] in the CB1R site is one in which the naphthoyl ring is nearly parallel to the XZ plane when the indole ring (pentyl chain pointing down) is in the XY plane.[15a,17,30] Further, for the indoles, it is the distal ring of the naphthoyl bicyclic system that has the role of binding stabilization by aromatic stacking interactions with the receptor pocket.[31] Hence, we prepared and tested the 2-phenylethylidene indene analogue (**2-7c**) wherein the naphthylidene ring was replaced with 2-phenylethylidene that retains only the distal aromatic ring in analogy with similar active indole analogues.[32] This change lost 10-fold affinity versus the corresponding naphthylidene analogue **2-7b** (both with an *n*-hexyl pendant group on inden-3-yl) and 256-fold versus **2-7a**, which carries a pentyl pendant group on inden-3-yl).

Reported studies on indenes that are conformationally restrained by an arylidene double bond indicate that it is the orientation defined by the E-geometry that is active in the indenes and, by extension, in the more conformationally mobile naphthoyl indoles.[17] Designing forward from these factors, other arrangements of arylidene rings on the indenes were synthesized and tested to evolve an SAR that mapped the regions proximal to the 1-naphthyl ring. Thus, fusing an additional phenyl ring to naphthylene gave the 5-phenanthrylidene ring (**2-5s**) (K_i = 22.9 nM) versus the naphylidene **2-5a** (4.69 nM), indicating a tolerence for the extra ligand volume. In contrast, an alternate fusing of a phenyl ring to a naphthyl ring in indoles to give the symmetrical 9-anthranoyl ring is reported to result in a significant loss of binding affinity.[31] This suggests that the volume available to the naphthoyl is not equivalent on both sides of the 9-anthranoyl bond to the indole and by extension to the indene.

Displacing the distal phenyl ring of the naphthylidene group of **2-5a** from the fused to a pendant arrangement as in a 2- or 3-phenylbenzylidene group (**2-5k** and **2-5e**, respectively) results in a reasonably tolerated receptor binding for hCB1R for **2-5k** (K_i = 82.9 nM) but not for **2-5e** (K_i = 2603 nM). Reorienting the 1-naphylidene ring to the 2-naphylidene ring (**2-5r**) (K_i = 134 nM) reduces binding affinity by a moderate extent.

Ortho-substituted benzylidene morpholinoethyl indenes were also synthesized and screened for hCB1R affinity based on the reported activity of 2-substituted benzoyl indoles.[15b] Versus the unsubstituted 2-protio analogue **2-5b** (K_i = 1297 nM), the 2-halogeno analogues (**2-5d,f,g,c**) (2-F, Cl, Br, I, respectively) showed increasing affinity (K_i = 1000, 862, 647, 607 nM, respectively) with larger halogen atoms but never rising to the effect of the much larger 2-phenylbenzylidene analogue (**2-5k**, K_i = 82.9 nM). The 2-methoxy substituent (**2-5h**, K_i = 149 nM) gave a large increase in binding affinity (vs **2-5b**) that was likely due to electronic issues given the similar enhancement in affinity seen for the 4-methoxynaphthylidene **2-5j** vs **2-5a**.

The affinity and possibly the functional bias of the receptor with its binding ligand can be influenced by the interaction of the arylidene or aroyl moieties of the indenes or the indoles, respectively. Modeling suggests that this interaction is one of aromatic stacking, which is effected by the electronic character of the interacting aromatic rings. Varying the arylidene ring systems to introduce electron-rich and electron-poor proximal or distal rings, we examined the effect on binding affinity. Thus, comparing the monocyclic electron-rich furanylidene **2-5n** (K_i

DOI: 10.1021/acs.jmedchem.6b00516
J. Med. Chem. 2016, 59, 7525−7543

Table 1. Compounds Key: Indoles (1) and Indenes (2)

compd	Z	R	$X_{1/2}$[a]	K_i (nM) hCB1R vs CP55,940
1-4a	H	Pn	CO_2Me	20.2
1-4b	H	H	CO_2Et	
1-4c	H	Pn	CO_2Et	115
1-4d	H	$(CH_2)_3$-CO_2Et	H	747
1-4e	H	$(CH_2)_4$-CO_2Et	H	1469
1-4f	H	$(CH_2)_3$-CO_2H	H	>10000
1-4g	H	$(CH_2)_4$-CO_2H	H	>10000
1-4h	4-F	Pn	H	6.5
1-4i	5-F	Pn	H	9.85
1-4j	6-F	Pn	H	2.35
1-4k	7-F	Pn	H	3.62
1-4l	4-F	5-F-Pn	H	4.38
1-4m	4-F	Et-Morp	H	237
1-4n	4-F	5-F-Pn	4-Pr	2.55
1-4o	H	Et-Morp	CO_2Me	52.4
1-4p	H	Pn	H	4.3 (15a)
1-7a	H	Pn	CO_2H	>10000
1-7b	H	Pn	CONHMe	127
1-7c	H	Pn	$CONH_2$	96.6
1-7d	H	Pn	COEt	5.71
1-7e	H	Pn, not prep	COMe	not tested
1-9a	H	Et-Morp	H	82
1-9b	H	Me, Et-Morp	H	>10000
1-9c	H	Et-Morp	OMe	88
1-9d	H	Me, Et-Morp	OMe	4083
1-9e	H	Et-Morp	Me	20
1-9f	H	Me, Et-Morp	Me	4174
1-9g		Et-Morp	pravadoline	2511 (rat)
1-9h		Me, Et-Morp	Me-pravadoline	>10000

compd	R	*E*-arylidene (morpholinoethyl indene)	W/X_1	K_i (nM) hCB1R vs CP55,940
2-5a ENMI	Et-Morp	1-naphthylidene	H	4.69 (2.72)
2-5b	Et-Morp	benzylidene	H	1297
2-5c	Et-Morp	2-iodobenzylidene	2-I	607
2-5d	Et-Morp	2-fluorobenzylidene	2-F	1000
2-5e	Et-Morp	3-phenylbenzylidene	3-Ph	2603
2-5f	Et-Morp	2-chlorobenzylidene	2-Cl	862
2-5g	Et-Morp	2-bromobenzylidene	2-Br	647
2-5h	Et-Morp	2-methoxybenzylidene	2-OMe	149
2-5i	Et-Morp	2-methylbenzylidene	2-Me	623
2-5j MoNMI	Et-Morp	4-methoxynaphthylidene	4-OMe	2.43
2-5k	Et-Morp	2-phenylbenzylidene	2-Ph	82.9
2-5l	Et-Morp	7-indolidene	H	107
2-5m	Et-Morp	2-thienylmethylene	H	8528
2-5n	Et-Morp	2-furanylmethylene	H	>10000
2-5o	Et-Morp	5-isoquinolidene	H	454
2-5p	Et-Morp	4-quinolidene	H	23.3
2-5q AceNMI	Et-Morp	1,2-dihydroacenaphthylidene-5-yl-methylene		15.9
2-5r	Et-Morp	2-naphthylidene		134
2-5s	Et-Morp	4-phenanthrylidene		22.9
2-5t EtNMI	Et-Morp	4-ethylnaphthylidene	Et	0.859
2-5u PrNMI	Et-Morp	4-propylnaphthylidene	Pr	1.18
2-5v	Et-Morp	1-naphthylidene (2-Me-indene)	H	2.84 (2.89)
2-6a	Me, Et-Morp	1-naphthylidene (indene)		982
2-6b	Me, Et-Morp	1-naphthylidene (2-Me-indene)		1614
2-7a	Pn	1-naphthylidene (indene)		17.2 (26)
2-7b	Hx	1-naphthylidene (indene)		436
2-7c	Hx	*E*-2-phenylethylidene		4414

[a]See Schemes 1 and 2 for X_1 and X_2

DOI: 10.1021/acs.jmedchem.6b00516
J. Med. Chem. 2016, 59, 7525−7543

Table 2. E-Arylidene Morpholinoethyl Indene Structures, hCB1R/hCB2R Binding, Permeability in the MDCK Cell Line Assay, Ca^{2+} Flux (hCB1R and hCB2R Agonist) Activity, and Metabolic Stability[a]

E-arylidene morpholinoethyl indene R-group					
Abbreviated name	EtNMI	PrNMI	MoNMI	ENMI	AceNMI
Structure Number	**2-5t**	**2-5u**	**2-5j**	**2-5a**	**2-5q**
CB1R Ki (nM)	0.86	1.18	2.43	4.17	15.9
CB2R Ki (nM)	0.79	1.00	4.07	5.62	4.22
MDCK B/A ratio	0.000	0.000	0.000	0.001	0.0014
hCB1R EC_{50} (nM)	141	182	196	257	--
hCB1R $\%E_{max}$	121	108	114	103	--
hCB2R EC_{50} (nM)	163	94	194	138	594
hCB2R $\%E_{max}$	59	69	52	27	20
% remaining in plasma at 1 hr	--	92	100	98.5	--
% remaining in S9 fraction at 1 hr	--	37	43	22.5	--

[a]--, not tested.

Table 3. Indole Core Structures, hCB1R/hCB2R Binding, Permeability in the MDCK Cell Line Assay, Ca^{2+} Flux (hCB1R agonist) Activity, and Metabolic Stability[a]

Indole structure	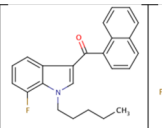	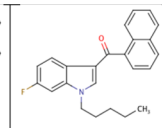	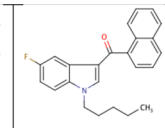	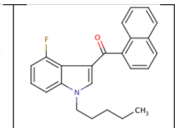
Structure Number	**1-4k**	**1-4j**	**1-4i**	**1-4h**
CB1R Ki (nM)	3.62	2.35	9.85	6.5
CB2R Ki (nM)	2.70	16.4	65.0	35.6
MDCK B/A ratio	0.000	0.000	0.000	0.000
hCB1R EC_{50} (nM)	104	--	--	--
hCB1R $\%E_{max}$	79	--	--	--
% remaining in plasma at 1 hr	97	80	99	69
% remaining in S9 fraction at 1 hr	50	30	13	5

[a]-- not tested.

= > 10 μM) to the electron-poor thiophenylidene **2-5m** (K_i = 8.5 μM), binding is favored by the electron-poor proximal ring. Similarly, comparing the bicyclic electron-poor 4-quinolidene **2-5p** (K_i = 23.3 nM) to the electron-neutral naphthylidene **2-5a** (K_i = 4.69 nM), binding is favored by the electron-neutral (or relatively electron-rich) proximal ring. Even though the binding by the electron-poor proximal ring was quite good, other factors such as interaction with the basic nitrogen atoms could contribute to the overall binding preference change toward electron density. Comparing the bicyclic electron-rich 7-indolydene **2-5l** (K_i = 107 nM) to the electron-poor 5-isoquinolidene **2-5o** (K_i = 454 nM), binding is favored by the electron-rich distal ring.

Given the ready metabolism of indoles, which not only leads to the consumption of the drug candidate but also to multiple metabolites that exhibit mixed pharmacologies,[33] the issue of stabilizing lead compounds was also addressed by introducing fluorine substitution on the indole ring to develop improved resistance to metabolism. The 4-, 5-, 6-, and 7-F indole analogues of **1-4p** (**1-4h**–**k**) all had K_is in the single-digit nM range. Tested for stability in rat plasma, where they exhibited stability of 69–99% after 1 h (see Table 3), and S9 plasma fraction, where stability increased from 3% to 50% in 1 h with F substitution going from positions 4 to 7. In our analogues, the indenes were more metabolically stable than the indoles.

In Vivo Efficacy of Indenes. We show that systemic (0.3 mg/kg, ip) administration of **2-5u** (**2-5u**) or **2-5j** (**2-5j**) produced complete suppression of mechanical allodynia symptoms (Figure 1B,C), while the same and 3-fold higher doses of these compounds had no effect in the assays of CNS CB1R activation compared to the brain-permeant positive control, **1** (Figure 2). Similarly, an oral dose of 3 mg/kg **2-5u** produced complete suppression of allodynia symptoms at peak effect, while a 10 mg/kg oral dose had no significant effect on central CB1Rs (Figure 2). These data support the high antiallodynic efficacy of indene-based peripherally restricted cannabinoids (PRCBs) at doses that do not produce any CNS side effects.

DOI: 10.1021/acs.jmedchem.6b00516
J. Med. Chem. 2016, 59, 7525–7543

The pharmacokinetic data, which showed a CSF:plasma ratio of 0.001 at ~75 min after **2**-**5u** (0.3 mg/kg, ip) administration (Figure 1E) supports its relative lack of brain permeability. Generally, increasing aqueous solubility decreases the likelihood of a drug gaining access to brain tissue. However, numerous lipid-soluble molecules, among them many useful therapeutic drugs, have lower brain permeability than would be predicted from a determination of their lipid solubility.[34] Given the very low aqueous solubility of PRCBs, their relative lack of BBB permeability suggests that they may be substrates for active drug efflux transporters such as P-glycoprotein or multidrug resistance proteins. Future studies using selective inhibitors of such transporters (e.g., ref 35) or transporter knockout rodents (e.g., ref 36) should help identify precisely the efflux transporters for which PRCBs serve as substrates.

We also demonstrated that PRCBs such as **2**-**5u** have small effects on acute nociception compared to the brain-permeable **1** in the tail-flick assay in naïve rats (Figure 2D,H,L), yet at the same doses exhibit potent antiallodynic effects in SNE neuropathy. Previous studies have demonstrated increases in expression of both CB1R and CB2R in sensory ganglia after inflammation and peripheral nerve injuries.[6a,37] Increases in CBR expression result in increased potency or efficacy of the exogenously applied CBs;[9] such increases may also account for the effectiveness of CBs in alleviating neuropathic pain symptoms after chronic repeated treatment.[10] Thus, increases in CB1R and CB2R expression may potentially account for the increased potency/efficacy of PRCBs after SNE injury. An alternative explanation for the increased efficacy of **2**-**5u** in SNE involves alterations in blood−nerve barrier (BNB) function. Many of the BBB efflux transporters are also involved in maintaining BNB function.[38] In normal conditions, these transporters may limit PRCB access to CBRs on nociceptors, which would account for the weak antinociceptive efficacy of PRCBs. However, there is growing evidence that chronic pain syndromes exhibit tissue abnormalities caused by microvasculature dysfunction in the blood vessels of skin, muscle, or nerve.[39] Such dysfunction, e.g., loosening of the tight junctions between the endoneurial endothelial cells,[38] may increase PRCB access to CBRs on sensory neurons, thereby increasing their effectiveness in suppressing painful neuropathy symptoms.

Our binding studies revealed similar affinities of **2**-**5u** and related indenes for the CB1R and CB2R subtypes. However, subsequent Ca^{2+} flux assays revealed that indene PRCBs are full agonists at hCB1R but only partial agonists at hCB2R (Table 2). In vivo, pretreatment with the CB2R-selective inverse agonist, **3** (Scheme 3), had only a small effect on suppression of allodynia by **2**-**5u**, while pretreatment with the brain-permeable CB1R-selective inverse agonist, rimonabant, or it is peripherally restricted analogue, **18A**,[27] prevented the antiallodynic effect of **2**-**5u** (Figure 3). These studies suggested that CB1Rs are mainly responsible for the antiallodynic effects of PRCBs. Previous studies with the brain-permeant synthetic CB, **4** (Scheme 3), which has full agonist activity at both CB1R and CB2R, demonstrated that its antiallodynic effects in some neuropathy models were mediated primarily by CB1R activation,[6c,10a,40] whereas in other models both CB1R and CB2R were involved.[12d,41] Further, our conclusions must be tempered by the fact that in vivo effects of inverse agonists such as rimonabant may be affected by changes in levels of endocannabinoids and their activation of CBRs in SNE neuropathy. Future studies using transgenic mice with deletions of CB1Rs and CB2Rs should be able to determine more precisely the relative contribution of CBR subtypes to the antiallodynic effects of PRCBs in different neuropathy models.

CONCLUSIONS

The hydrophobic PRCB compounds, which we developed, are the first in their class of high peripheral selectivity CB1R agonists to exhibit, after systemic or oral administration, potent, and repeated suppression of neuropathy symptoms with a lack of side effects mediated by activation of central CB1 receptors. The potency, peripheral selectivity, in vivo efficacy, and absence of CNS side effects of the PRCBs hold promise as a viable treatment for neuropathic pain states.

EXPERIMENTAL METHODS

General. ^{1}H and ^{13}C NMR spectra were run on a Bruker Avance 300 MHz or a Varian Unity Inova 500 MHz NMR spectrometer. Mass spectra (MS) were run on a PerkinElmer Sciex API 150 EX mass spectrometer. High resolution mass spectra (HRMS) were run on a Waters Synapt G2 Q-TOF mass spectrometer in high-resolution mode. Column chromatography was carried out using a Teledyne Isco Combiflash Rf system with RediSep Rf silica cartridges. Preparative thin layer chromatography was carried out using Analtech TLC Uniplates (silica gel, 1000 mm, 20 cm × 20 cm). High pressure liquid chromatography was performed using a system consisting of a Waters 1525 pump unit, driven by Empower software, and a Waters 2487 detector. Microwave chemistry was carried out using a CEM Discover SP microwave with 10 mL irradiation tubes.

*4-Propylnaphthalene-1-carbonyl Chloride (**1**-**2b**).* 4-Propylnaphthalene-1-carboxylic acid (500 mg, 2.33 mmol) was dissolved in dichloromethane (15 mL) and cooled to 0 °C in an ice bath. Oxalyl chloride (1.49 g) was then added dropwise over 5 min. Once the addition was complete, the mixture was allowed to stir at room temperature for 45 min and then under reflux for 45 min. The solution was then cooled to room temperature. Removal of the solvent afforded 4-propylnaphthalene-1-carbonyl chloride (**1**-**2b**), which was used in the preparation of **1**-**3f** without further purification (assuming 542 mg, 100%).

*Methyl 4-[(1H-Indol-3-yl)carbonyl]naphthalene-1-carboxylate (**1**-**3b**).* Indole (**1**-**1**) (8.12 g, 98%, 0.068 mol) was dissolved in dichloromethane (150 mL), purged with nitrogen, and cooled to 0 °C in an ice bath. Methylmagnesium bromide (0.023 L, 3 M in ether, 0.069 mol) was added to the solution over 10 min and mixture stirred for an additional 10 min at 0 °C. Powdered $ZnCl_2$ (31.3 g, solid addition funnel) and anhydrous ether (80 mL, addition funnel) were then added over 10 min and the mixture stirred for an additional 10 min at 0 °C. The solution was allowed to warm to room temperature and stirred for 30 min. Methyl 4-(carbonochloridoyl)naphthalene-1-carboxylate (**1**-**2a**) (17.24 g, 0.069 mol) in CH_2CL_2 (80 mL) was then added over several minutes and the solution stirred at room temperature overnight. Subsequently, saturated aqueous ammonium chloride solution (80 mL) was added and the mixture stirred for 15 min. The solid was removed by filtration and washed with water and ether. This solid was vacuumed dried to give the title product (11.97 g). The organic and aqueous layers of the filtrate were then separated. The organic layer was then washed with water, dried over sodium sulfate, and the solvent removed under reduced pressure. The residue was then triturated with a small amount of ether. The solid was removed by filtration and vacuumed dried to give additional product (8.36 g, 20.33 g total, 91%). ^{1}H NMR (300 MHz, $CDCl_3$) δ 4.05 (s, 3H), 7.31−7.52 (m, 5H), 7.58−7.67 (m, 2H), 8.12 (d, J = 8.4 Hz, 1H), 8.18 (d, J = 7.4 Hz, 1H), 8.45−8.52 (m, 1H), 8.78 (br s, 1H), 8.91 (d, J = 8.6 Hz, 1H).

*X-Fluoro-3-[(naphthalen-1-yl)carbonyl]-1H-indole (X = 4−7) (**1**-**3e**−**h**).* These analogues were prepared by a similar method described for **1**−**3b** with variations of additional further extractions of the aqueous layer with ether or dichloromethane, drying, and trituration in dichloromethane or ether.

*4-Fluoro-3-[(naphthalen-1-yl)carbonyl]-1H-indole (**1**-**3e**).* 4-Fluoroindole (**1**-**1b**) (2.03 g, 0.0147 mol) was dissolved in dichloromethane

DOI: 10.1021/acs.jmedchem.6b00516
J. Med. Chem. 2016, 59, 7525−7543

(60 mL) and cooled to 0 °C in an ice bath. Methylmagnesium bromide (0.005 L, 3 M in ether, 0.015 mol) was added to the solution, under nitrogen, over 5 min. The mixture was then stirred for 10 min at 0 °C, $ZnCl_2$ solution (0.0049 L, 1 M in ether, 0.0496 mol) added dropwise over 10 min, and the mixture stirred for an additional 10 min at 0 °C. The solution was allowed to warm to room temperature and stir for 30 min. 1-Naphthoyl chloride (**1-2e**) (0.002 L, 97%, 0.015 mol) was then added over several minutes and the solution stirred at room temperature overnight. Subsequently, saturated aqueous ammonium chloride solution (120 mL) was added and the mixture stirred for 30 min. The precipitate was removed by filtration, washed well with water, and dried under vacuum to give the title compound as an off-white solid (3.40 g, 80%). ^{1}H NMR (300 MHz, DMSO-d_6) δ 6.95−7.05 (m, 1H), 7.23−7.33 (m, 1H), 7.38 (d, J = 8.0 Hz, 1C), 7.48−7.62 (m, 3H), 7.65−7.73 (m, 2H), 8.00−8.13 (m, 3H), 8.08−8.17 (m, 2H), 12.30 (s, 1H). ^{13}C NMR (75.5 MHz, DMSO-d_6) δ 107.51 (d, J = 20.8 Hz, 1C), 108.82 (d, J =J = 3.8 Hz, 1C), 113.37 (d, J = 21.2 Hz, 1C), 117.20 (d, J = 5.9 Hz, 1C), 124.15 (d, J = 7.5 Hz, 1C), 124.80, 125.28, 126.20 (2C), 126.75, 128.28, 129.91, 130.25, 133.25, 137.22, 138.81 (d, J = 2.3 Hz, 1C), 140.03 (d, J = 11.4 Hz, 1C), 155.88 (d, J = 251.0 Hz, 1C), 189.48.

*5-Fluoro-3-[(naphthalen-1-yl)carbonyl]-1H-indole (**1-3f**).* Off-white solid (3.37 g, 85%). ^{1}H NMR (300 MHz, DMSO-d_6) δ 7.11−7.22 (m, 1H), 7.48−7.67 (m, 4H), 7.68−7.75 (m, 1H), 7.78 (s, 1H), 7.94−8.14 (m, 4H), 12.20 (s, 1H). ^{13}C NMR (75.5 MHz, DMSO-d_6) δ 106.28 (d, J = 24.6 Hz, 1C), 111.39 (d, J = 26.0 Hz, 1C), 113.71 (d, J = 9.8 Hz, 1C), 117.17 (d, J = 4.4 Hz, 1C), 124.88, 125.22, 125.73, 126.25, 126.44 (d, J = 11.0 Hz, 1C), 126.74, 128.27, 129.78, 129.99,133.29, 133.56, 138.01, 138.23, 158.83 (d, J = 234.9 Hz, 1C), 191.17.

*6-Fluoro-3-[(naphthalen-1-yl)carbonyl]-1H-indole (**1-3g**).* Light-pink solid (3.42 g total, 80%). ^{1}H NMR (300 MHz, DMSO-d_6) δ 7.11−7.22 (m, 1H), 7.30−7.38 (m, 1H), 7.48−7.66 (m, 3H), 7.67−7.76 (m, 2H), 7.97−8.06 (m, 2H), 8.10 (d, J = 8.1 Hz, 1H), 8.25−8.36 (m, 1H), 12.12 (s, 1H). ^{13}C NMR (75.5 MHz, DMSO-d_6) δ 98.67 (d, J = 25.8 Hz, 1C), 110.44 (d, J = 23.9 Hz, 1C), 117.10, 122.52 (d, J = 1.7 Hz, 1C), 122.66, 124.86, 125.23, 125.75, 126.24, 126.74, 128.27, 129.76, 130.01, 133.28, 137.08 (d, J = 12.5 Hz, 1C), 137.35 (d, J = 1.9 Hz, 1C), 138.25, 159.46 (d, J = 237.4 Hz, 1C), 191.23.

*7-Fluoro-3-[(naphthalen-1-yl)carbonyl]-1H-indole (**1-3h**).* White solid (1.51 g total, 72%). ^{1}H NMR (300 MHz, DMSO-d_6) δ 7.11−7.21 (m, 1H), 7.22−7.32 (m, 1H), 7.49−7.68 (m, 3H), 7.70−7.78 (m, 2H), 8.00−8.07 (m, 2H), 8.08−8.17 (m, 2H), 12.68 (s, 1H). ^{13}C NMR (75.5 MHz, DMSO-d_6) δ 108.30 (d, J = 15.8 Hz, 1C), 117.56 (d, J = 3.5 Hz, 1C), 117.91 (d, J = 1.3 Hz, 1C), 122.80 (d, J = 6.0 Hz, 1C), 124.76 (d, J = 13.3 Hz, 1C), 124.89, 125.19, 125.92, 126.26, 126.78, 128.30, 129.47 (d, J = 4.6 Hz, 1C), 129.92, 129.99, 133.31, 137.06, 138.18, 149.12 (d, J = 245.1 Hz, 1C), 191.34.

*4-Fluoro-3-[(4-propylnaphthalen-1-yl)carbonyl]-1H-indole (**1-3i**).* 4-Fluoroindole (**1-1b**) (1.47 mmol), methylmagnesium bromide (2.4 mmol), $ZnCl_2$ solution (1 M in ether, 8.0 mmol), and 4-propylnaphthalene-1-carbonyl chloride[32] (**1-2b**) (2.33 mmol) were similarly processed as for **1-3b**. White solid (440 mg total, 58%). ^{1}H NMR (300 MHz, DMSO-d_6) δ 1.02 (t, J = 7.3 Hz, 3C), 1.67−1.82 (m, 2H), 3.09 (t, J = 7.4 Hz, 2C), 6.92−7.02 (m, 1H), 7.20−7.31 (m, 1H), 7.36 (d, J = 8.0 Hz, 1H), 7.42 (d, J = 7.2 Hz, 1H), 7.47−7.63 (m, 3H), 7.66 (s, 1H), 8.09 (d, J = 8.1 Hz, 1H), 8.17 (d, J = 8.3 Hz, 1H), 12.30 (s, 1H). ^{13}C NMR (75.5 MHz, DMSO-d_6) δ 13.99, 23.45, 34.47, 107.41 (d, J = 20.8 Hz, 1C), 108.80 (d, J = 3.7 Hz, 1C), 113.44 (d, J = 21.1 Hz, 1C), 117.31 (d, J = 5.9 Hz, 1C), 124.03 (d, J = 7.7 Hz, 1C), 124.12, 124.73, 126.07 (3C), 126.22, 130.75, 131.58, 137.00, 137.28 (d, J = 2.4 Hz, 1C), 140.02 (d, J = 11.4 Hz, 1C), 140.60, 155.90 (d, J = 251.1 Hz, 1C), 189.63.

*Methyl 4-[(1-Pentyl-1H-indol-3-yl)carbonyl]naphthalene-1-carboxylate (**1-4a**).* DMF (15 mL) was cooled to 0 °C, and sodium hydride (245 mg, 60% in mineral oil, 6.1 mmol) added over a few minutes. After the addition was complete, the mixture was stirred for an additional 10 min before adding a solution of methyl 4-[(1*H*-Indol-3-yl)carbonyl]naphthalene-1-carboxylate (**1-3b**) (1 g, 0.003 mol) in DMF (15 mL) dropwise. The solution was then stirred for 30 min at 0 °C. A solution of pentyl bromide (0.415 mL) in DMF (8 mL) was added and the mixture allowed to warm to room temperature and stirred overnight. The solvent was removed under reduced pressure and EtOAc (25 mL) and water (25 mL) added to the residue. The mixture was shaken and the organic layer removed and washed with water. The solvent was removed under reduced pressure and residue was columned over silica gel (Isco, gradient from 100% hexane to 30% EtOAc/70% hexane) to give the title product as an off-white solid (630 mg, 52%). ^{1}H NMR (300 MHz, $CDCl_3$) δ 0.84 (t, J = 6.6 Hz, 3H), 1.17−1.37 (m, 4H), 1.72−1.88 (m, 2H), 3.98−4.10 (m, 5H), 7.23−7.29 (m, 1H), 7.32−7.43 (m, 3H), 7.44−7.54 (m, 1H), 7.68−7.78 (m, 2H), 8.09−8.17 (m, 1H), 8.20 (d, J = 7.4 Hz, 1H), 8.42−8.50 (m, 1H), 8.92 (d, J = 8.5 Hz, 1H).

*Ethyl 4-[(1H-Indol-3-yl)carbonyl]naphthalene-1-carboxylate (**1-4b**) and Ethyl 4-[(1-Pentyl-1H-indol-3-yl)carbonyl]naphthalene-1-carboxylate (**1-4c**).* DMF (150 mL) was cooled to 0 °C and sodium hydride (3.68 g, 60% in mineral oil, 0.092 mol) was added over several minutes. The mixture was then stirred for an additional 10 min, and a solution of methyl 4-[(1*H*-Indol-3-yl)carbonyl]naphthalene-1-carboxylate (**1-3b**) (15 g, 0.046 mol) in DMF (150 mL) was added dropwise. The solution was then stirred for 30 min at 0 °C. A solution of pentyl bromide (7.56 g, 0.05 mol) in DMF (75 mL) was added and the mixture allowed to warm to room temperature and stir overnight. The solvent was removed, EtOAc (100 mL) added to the residue, and the inorganic solid removed by filtration. Water (100 mL) was then added to the filtrate and the mixture stirred for 10 min. The organic layer was removed, dried over sodium sulfate, and the solvent removed under reduced pressure. The residue was purified over silica gel (Isco, gradient from 100% hexane to 30% EtOAc/70% hexane) to give the title compounds via transesterification as light-yellow solids.

*Ethyl 4-[(1H-Indol-3-yl)carbonyl]naphthalene-1-carboxylate (**1-4b**).* Yield (3.0 g, 19%). ^{1}H NMR (300 MHz, $CDCl_3$) δ 1.49 (t, J = 7.1 Hz, 3H), 4.52 (q, J = 7.1 Hz, 2H), 7.26 (s, 1H), 7.28−7.49 (m, 4H), 7.54−7.65 (m, 2H), 8.09 (d, J = 8.5 Hz, 1H), 8.15 (d, J = 7.4 Hz, 1H), 8.89 (d, J = 8.7 Hz, 1H), 8.89 (d, J = 8.7 Hz, 1H), 9.08 (broad s, 1H). ^{13}C NMR (75.5 MHz, $CDCl_3$) δ 14.40, 61.41, 11.60, 118.93, 122.56, 123.23, 123.77, 124.28, 125.73, 125.93, 126.29, 126.95, 127.93, 128.50, 129.23, 131.06, 131.52, 135.25, 136.60, 142.23, 167.40, 192.11.

*Ethyl 4-[(1-Pentyl-1H-indol-3-yl)carbonyl]naphthalene-1-carboxylate (**1-4c**).* Yield (6.7 g, 36%). ^{1}H NMR (300 MHz, $CDCl_3$) δ 0.84 (t, J = 6.8 Hz, 3H), 1.16−1.36 (m, 4H), 1.49 (t, J = 7.1 Hz, 3H), 1.71−1.85 (m, 2H), 4.04 (t, J = 7.2 Hz, 2H), 4.52 (q, J = 7.1 Hz, 2H), 7.27 (s, 1H), 7.32−7.45 (m, 3H), 7.46−7.53 (m, 1H), 7.58−7.69 (m, 2H), 8.14 (d, J = 8.2 Hz, 1H), 8.19 (d, J = 7.1 Hz, 1H), 8.43−8.53 (m, 1H) 8.92 (d, J = 8.6 Hz, 1H). ^{13}C NMR (75.5 MHz, $CDCl_3$) δ 13.84, 14.43, 22.15, 28.91, 29.45, 47.26, 61.36, 110.08, 117.41, 122.91, 123.10, 123.72, 123.81, 125.92, 126.48, 126.79, 126.87, 127.91, 128.59, 129.01, 131.18, 131.57, 137.12, 138.09, 143.65, 167.47, 191.31. HPLC 97% (Waters X-Bridge C-18 5 μm, 4.6 mm × 100 mm column, 10 mM aqueous NH_4OAc-CH_3CN, 40:60, UV detection at 254 nm). HRMS: calculated for $C_{27}H_{28}NO_3$ (M + H) 414.2069, found 414.2063 (M + H).

*N-(3-Ethoxycarbonylpropyl)-3-(1-naphthoyl)-1H-indole (**1-4d**).* To a vacuum-dried flask under N_2 was added NaH (60% dispersion in oil, 9.1 mmol, 0.37 mg) and the flask was cooled to 0 °C and dry DMF (29 mL) was added. The mixture was stirred for 10 min and a solution of 3-(1-naphthoyl)indole[16] (2.0 g, 0.00729 mol) in DMF (28 mL) was added dropwise over 30 min. After complete addition, the mixture was stirred an additional 30 min and then a solution of ethyl bromobutyrate (3.55 g, 0.0182 mol) in 14 mL of DMF was added over 15 min and the reaction mixture was allowed to warm to room temperature overnight. TLC (SiO_2; hexane/EtOAc (10:1)) showed the consumption of starting material. The DMF was removed under reduced pressure, and the resulting residue was partitioned between water (100 mL) and EtOAc (3 × 100 mL) followed by CH_2Cl_2 (2 × 100 mL). The organics were combined, the solvent removed in vacuo, and the residual material was chromatographed on an Isco 80 g silica column eluting with a gradient from hexanes (100%) to hexane/EtOAc (7:3) that afforded the desired compound in 92% yield. ^{1}H NMR (300 MHz, $CDCl_3$) δ 1.08 (t, J = 7.13 Hz, 3H), 1.93−2.08 (m, 2H), 2.10−2.22 (m, 2H), 3.91−4.11 (m, 4H), 7.19−7.48 (m, 7H), 7.55 (d, J = 6.9 Hz, 1H), 7.80 (d, J = 7.5 Hz, 1H), 7.86 (d, J = 8.2 Hz, 1H), 8.09 (d, J = 8.0 Hz, 1H), 8.37−8.47 (m, 1H). ^{13}C NMR (75.5 MHz, $CDCl_3$) δ 14.11, 24.97, 30.77, 46.05, 60.68, 109.92, 117.89, 122.98, 123.01, 123.80, 124.54, 125.82, 125.95,

DOI: 10.1021/acs.jmedchem.6b00516
J. Med. Chem. 2016, 59, 7525−7543

126.28, 126.76, 127.01, 128.17, 130.01, 130.79, 133.77, 137.00, 137.80, 139.00, 172.31, 192.00.

*N-(3-Ethoxycarbonylbutyl)-3-(1-naphthoyl)-1H-indole (**1-4e**).* Prepared as for the ethoxycarbonylpropyl analogue **1-4d** from ethyl bromovalerate (0.160 mL, 1.014 mmol) afforded 85% of the title compound. ^{1}H NMR (300 MHz, $CDCl_3$) δ 1.09 (t, J = 7.1 Hz, 3H), 1.41−1.55 (m, 2H), 1.65−1.81 (m, 2H), 2.16 (t, J = 7.2 Hz, 3H), 3.90−4.06 (m, 4H), 7.21−7.48 (m, 7H), 7.55 (d, J = 7.0 Hz, 1H), 7.79 (d, J = 7.7 Hz, 1H), 7.85 (d, J = 8.2 Hz, 1H), 8.09 (d, J = 8.1 Hz, 1H), 8.36−8.44 (m, 1H). ^{13}C NMR (75.5 MHz, $CDCl_3$) δ 14.17, 22.14, 29.21, 33.52, 46.82, 60.43, 109.87, 117.77, 122.91, 123.02, 123.70, 124.56, 125.84, 125.98, 126.28, 126.75, 127.05, 128.17, 129.98, 130.81, 133.78, 136.99, 137.69, 139.07, 172.81, 191.97

*N-(3-Carboxypropyl)-3-(1-naphthoyl)-1H-indole (**1-4f**).* Ester **1-4d** (50 mg) was then treated with sodium hydroxide and water:methanol (1:1) mixture and heated to 50 °C for 2 h. Cooling and treatment with 2 N HCl, extraction with ethyl acetate, and drying with magnesium sulfate followed by filtration and concentration provided the desired acid for testing purposes in yields of 96%. ^{1}H NMR (300 MHz, $_3$acetonitrile-d_3) δ 1.96−2.10 (m, 2H), 2.17−2.29 (m, 2H), 4.19 (d, J = 7.1 Hz, 2H), 7.30−7.43 (m, 2H), 7.46−7.63 (m, 5H), 7.67−7.75 (m, 1H), 7.95−8.14 (m, 3H), 8.36−8.46 (m, 1H). ^{13}C NMR (75.5 MHz, acetonitrile-d_3) δ 24.44, 29.66, 45.47, 110.35, 116.70, 121.84, 122.35, 123.23, 124.55, 125.26, 125.64, 126.01, 126.41, 126.64, 127.97, 129.46, 130.27, 133.46, 136.91, 138.69, 138.75, 172.89, 191.34. EIMS: calculated for $C_{23}H_{19}NO_3$ 357.40, found 358.4 (M + H).

*N-(3-Carboxybutyl)-3-(1-naphthoyl)-1H-indole (**1-4g**).* Prepared as for the above carboxypropyl analogue from the corresponding ester in 78% yield. ^{1}H NMR (300 MHz, $CDCl_3$) δ 1.45−1.58 (m, 2H), 1.71−1.84 (m, 2H), 2.24 (t, J = 7.2 Hz, 2H), 3.97−4.05 (m, 2H), 7.24−7.48 (m, 7H), 7.57 (d, J = 6.7 Hz, 1H), 7.78−7.92 (m, 2H), 8.10 (d, J = 8.1 Hz, 1H), 8.37−8.44 (m, 1H). ^{13}C NMR (75.5 MHz, $CDCl_3$) δ 21.84, 29.11, 33.14, 46.75, 109.85, 117.77, 122.97, 123.01, 123.74, 124.56, 125.87, 125.94, 126.26, 126.76, 127.00, 128.17, 130.03, 130.77, 133.74, 136.97, 137.77, 138.96, 178.13, 192.14. EIMS: calculated for $C_{24}H_{21}NO_3$ 371.43, found 372.1 (M + H).

*X-Fluoro-3-[(naphthalen-1-yl)carbonyl]-1-alkyl-1H-indole (X = 4−7) (**1-4h−m**).* These analogues were prepared by the same method described for **1-4h** on the same or 55, 55, 59, and 25% scale (**1-4k−n**).

*4-Fluoro-3-[(naphthalen-1-yl)carbonyl]-1-pentyl-1H-indole (**1-4h**).* Sodium hydride (207 mg, 60% in oil, 5.18 mmol) was added to DMF (20 mL) at 0 °C and the mixture stirred for 10 min. A solution of 4-fluoro-3-[(naphthalen-1-yl)carbonyl]-1*H*-indole (**1-3e**) (750 mg, 2.59 mmol) in DMF (10 mL) was added dropwise over 5 min and the resulting solution stirred at 0 °C for 30 min. A solution of 1-bromopentane (431 mg, 2.85 mmol) in DMF (1 mL) was then added dropwise to the stirred mixture. Cooling was continued for an additional 10 min before allowing the solution to warm to room temperature and stir overnight. The reaction was quenched with water (75 mL), and EtOAc (50 mL) was added. The mixture was shaken and the organic layer removed. The aqueous layer was then extracted with additional EtOAc (50 mL). The organic layers were combined, dried over Na_2SO_4, and the solvent removed under reduced pressure. The residue was purified over silica gel (Isco, 120 g column, gradient from 100% hexane to 30% EtOAc/70% hexane) to give the title compound as a colorless resin (760 mg, 82%). ^{1}H NMR (300 MHz, $CDCl_3$) δ 0.85 (t, J = 6.8 Hz, 3H), 1.15−1.38 (m, 4H), 1.72−1.87 (m, 2H), 4.04 (t, J = 7.2 Hz, 2H), 6.93−7.03 (m, H), 7.16 (d, J = 8.0 Hz, 1H), 7.22−7.30 (m, 1H), 7.33 (s, 1H), 7.43−7.55 (m, 3H), 7.63−7.70 (m, 1H), 7.85−7.93 (m, 1H), 7.97 (d, J = 8.3 Hz, 1H), 8.23−8.31 (m, 1H). ^{13}C NMR (75.5 MHz, $CDCl_3$) δ 13.83, 22.14, 28.86, 29.32, 47.43, 106.11 (d, J = 4.1 Hz, 1C), 108.48 (d, J = 21.5 Hz, 1C), 114.91 (d, J = 21.2 Hz, 1C), 117.64 (d, J = 5.8 Hz, 1C), 124.33 (d, J = 8.0 Hz, 1C), 124.41, 126.08, 126.26, 126.75, 126.86, 128.18, 130.40, 131.07, 133.74, 138.12, 139.09 (d, J = 2.7 Hz, 1C), 139.91 (d, J = 11.0 Hz, 1C), 157.03 (d, J = 254.0 Hz, 1C), 190.34. HPLC 99% (Waters X-Bridge C-18 5 μm, 4.6 mm × 100 mm column, H_2O−CH_3CN, 35:65, UV detection at 254 nm). HRMS: calculated for $C_{24}H_{23}NOF$ (M + H) 360.1764, found 360.1760 (M + H).

*5-Fluoro-3-[(naphthalen-1-yl)carbonyl]-1-pentyl-1H-indole (**1-4i**).* Colorless resin (760 mg, 81%). ^{1}H NMR (300 MHz, $CDCl_3$) δ 0.85 (t, J = 6.8 Hz, 3H), 1.17−1.38 (m, 4H), 1.71−1.88 (m, 2H), 4.05 (t, J = 7.2 Hz, 2H), 7.04−7.14 (m, 2H), 7.37 (s, 1H), 7.43−7.57 (m, 3H), 7.61−7.68 (m, 1H), 7.87−7.94 (m, 1H), 7.98 (d, J = 8.2 Hz, 1H), 8.13−8.21 (m, 1H), 8.39−8.48 (m, 1H). ^{13}C NMR (75.5 MHz, $CDCl_3$) δ 13.83, 22.14, 28.89, 29.48, 47.46, 108.33 (d, J = 24.8 Hz, 1C), 110.76 (d, J = 9.8 Hz, 1C), 112.00 (d, J = 26.7 Hz, 1C), 117.50 (d, J = 4.5 Hz, 1C), 124.54, 125.82, 125.91, 126.36, 126.84, 127.75 (d, J = 11.7 Hz, 1C), 128.21, 130.12, 130.76, 133.57, 133.80, 138.68, 138.84, 159.92 (d, J = 238.7 Hz, 1C), 191.73. HPLC 99% (Waters X-Bridge C-18 5 μm, 4.6 mm × 100 mm column, H_2O−CH_3CN, 35:65, UV detection at 254 nm). HRMS: calculated for $C_{24}H_{23}NOF$ (M + H) 360.1764, found 360.1763 (M + H).

*6-Fluoro-3-[(naphthalen-1-yl)carbonyl]-1-pentyl-1H-indole (**1-4j**).* Colorless resin (840 mg, 90%). ^{1}H NMR (300 MHz, $CDCl_3$) δ 0.85 (t, J = 6.8 Hz, 3H), 1.18−1.40 (m, 4H), 1.72−1.87 (m, 2H), 4.00 (t, J = 7.2 Hz, 2H), 7.02−7.16 (m, 2H), 7.32 (s, 1H), 7.43−7.58 (m, 3H), 7.61−7.69 (m, 1H), 7.87−7.95 (m, 1H), 7.98 (d, J = 8.2 Hz, 1H), 8.14−8.22 (m, 1H), 8.39−8.48 (m, 1H). ^{13}C NMR (75.5 MHz, $CDCl_3$) δ 13.82, 22.15, 28.88, 29.35, 47.32, 96.64 (d, J = 26.9 Hz, 1C), 111.34 (d, J = 23.9 Hz, 1C), 117.70, 123.38, 124.09 (d, J = 10.1 Hz, 1C), 124.51, 125.89, 125.93, 126.35, 126.83, 128.21, 130.13, 130.80, 133.79, 137.31 (d, J = 11.6 Hz, 1C), 138.13 (d, J = 2.9 Hz, 1C), 138.83, 160.57 (d, J = 241.0 Hz, 1C), 191.88. HPLC 99% (Waters X-Bridge C-18 5 μm, 4.6 mm × 100 mm column, H_2O−CH_3CN, 35:65, UV detection at 254 nm). HRMS: calculated for $C_{24}H_{23}NOF$ (M + H) 360.1764, found 360.1758 (M + H).

*7-Fluoro-3-[(naphthalen-1-yl)carbonyl]-1-pentyl-1H-indole (**1-4k**).* Colorless resin (430 mg, 83%). ^{1}H NMR (300 MHz, $CDCl_3$) δ 0.85 (t, J = 6.7 Hz, 3H), 1.17−1.38 (m, 4H), 1.72−1.88 (m, 2H), 4.20 (t, J = 7.2 Hz, 2H), 6.97−7.08 (m, 1H), 7.20−7.31 (m, 2H), 7.43−7.58 (m, 3H), 7.61−7.68 (m, 1H), 7.87−7.94 (m, 2H), 8.13−8.21 (m, 1H), 8.27 (d, J = 8.0 Hz, 1H). ^{13}C NMR (75.5 MHz, $CDCl_3$) δ 13.84, 22.14, 28.65, 30.83 (d, J = 2.0 Hz, 1C), 50.0 (d, J = 5.1 Hz, 1C), 109.47 (d, J = 18.2 Hz, 1C), 118.02, 118.67 (d, J = 3.6 Hz, 1C), 123.31 (d, J = 6.5 Hz, 1C), 124.54, 124.88 (d, J = 7.5 Hz, 1C), 125.91 (2C), 126.37, 126.86, 128.22, 130.18, 130.72, 130.76, 133.79, 138.89, 139.08, 149.89 (d, J = 245.3 Hz, 1C), 191.89. HPLC 99% (Waters X-Bridge C-18 5 μm, 4.6 mm × 100 mm column, H_2O−CH_3CN, 35:65, UV detection at 254 nm). HRMS: calculated for $C_{24}H_{23}NOF$ (M + H) 360.1764, found 360.1763 (M + H).

*4-Fluoro-1-(5-fluoropentyl)-3-[(naphthalen-1-yl)carbonyl]-1H-indole (**1-4l**).* Colorless resin (150 mg, 28%). ^{1}H NMR (300 MHz, $CDCl_3$) δ 1.32−1.46 (m, 2H), 1.55−1.76 (m, 2H), 1.77−1.92 (m, 2H), 4.07 (t, J = 7.2 Hz, 2H), 4.29 (t, J = 7.2 Hz, 1H), 4.45 (t, J = 5.8 Hz, 1H), 6.93−7.03 (m, 1H), 7.16 (d, J = 8.1 Hz, 1H), 7.22−7.31 (m, 1H), 7.33 (s, 1H), 7.43−7.55 (m, 3H), 7.63−7.69 (m, 1H), 7.85−7.92 (m, 1H), 7.96 (d, J = 8.2 Hz, 1H), 8.22−8.29 (m, 1H). ^{13}C NMR (75.5 MHz, $CDCl_3$) δ 22.76 (d, J = 4.9 Hz, 1C), 29.31, 29.82 (d, J = 19.8 Hz, 1C), 47.27, 83.51(d, J = 165.1 Hz, 1C), 106.04 (d, J = 4.0 Hz, 1C), 108.54 (d, J = 21.3 Hz, 1C), 114.92 (d, J = 21.2 Hz, 1C), 117.79 (d, J = 5.8 Hz, 1C), 124.43, 124.45 (d, J = 7.8 Hz, 1C), 126.04, 126.28, 126.79, 126.87, 128.21, 130.46, 131.05, 133.75, 137.99, 139.00 (d, J = 2.8 Hz, 1C), 139.85 (d, J = 11.0 Hz, 1C), 157.05 (d, J = 254.3 Hz, 1C), 190.31. HPLC 98% (Waters X-Bridge C-18 5 μm, 4.6 mm × 100 mm column, H_2O−CH_3CN, 35:65, UV detection at 254 nm). HRMS: calculated for $C_{24}H_{22}NOF_2$ (M + H) 378.1669, found 378.1671 (M + H).

*4-Fluoro-1-[2-(morpholin-4-yl)ethyl]-3-[(naphthalen-1-yl)-carbonyl]-1H-indole (**1-4m**).* Light-yellow liquid (420 mg, 69%). ^{1}H NMR (300 MHz, $CDCl_3$) δ 2.34 (t, J = 4.6 Hz, 4H), 2.65 (t, J = 6.2 Hz, 2H), 3.49 (t, J = 4.5 Hz, 4H), 4.11 (t, J = 6.2 Hz, 2H), 6.95−7.04 (m, 1H), 7.15 (d, J = 8.1 Hz, 1H), 7.21−7.32 (m, 1H), 7.42 (s, 1H), 7.39−7.55 (m,3H), 7.62−7.69 (m, 1H), 7.86−7.93 (m, 1H), 7.96 (d, J = 8.0 Hz, 1H), 8.19−8.27 (m, 1H). ^{13}C NMR (75.5 MHz, $CDCl_3$) δ 42.10, 51.32 (2C), 55.01, 64.54 (2C), 103.57 (d, J = 3.8 Hz, 1C), 106.39 (d, J = 21.3 Hz, 1C), 112.48 (d, J = 21.3 Hz, 1C), 115.46 (d, J = 5.9 Hz, 1C), 122.13, 122.25, 123.79, 124.06, 124.27, 124.62, 125.97, 128.07, 128.77, 131.48, 136.91 (d, J = 2.7 Hz, 1C), 137.12, 137.70 (d, J = 11.1 Hz, 1C), 154.85 (d, J = 254.3 Hz, 1C), 188.03. HPLC 99% (Waters X-Bridge C-18 5 μm, 4.6 mm × 100 mm column, 10 mM aqueous NH_4OAc-

DOI: 10.1021/acs.jmedchem.6b00516
J. Med. Chem. 2016, 59, 7525−7543

CH_3CN, 45:55, UV detection at 254 nm). HRMS: calculated for $C_{25}H_{24}N_2O_2F$ (M + H) 403.1822, found 403.1830 (M + H).

*4-Fluoro-1-(5-fluoropentyl)-3-[(4-propylnaphthalen-1-yl)-carbonyl]-1H-indole (**1-4n**).* Light-yellow liquid (68 mg, 24%). ^{1}H NMR (300 MHz, $CDCl_3$) δ 1.06 (t, J = 7.3 Hz, 3H), 1.33−1.46 (m, 2H), 1.56−1.75 (m, 2H), 1.76−1.91 (m, 4H), 3.11 (t, J = 7.5 Hz, 2H), 4.07 (t, J = 7.1 Hz, 2H), 4.30 (t, J = 5.8 Hz, 1H), 4.46 ((t, J = 5.9 Hz, 1H), 6.94−7.03 (m, 1H), 7.16 (d, J = 8.1 Hz, 1H), 7.23−7.29 (m, 1H), 7.30−7.37 (m, 2H), 7.43−7.57 (m, 2H), 7.58−7.62 (m, 2H), 8.11 (d, J = 8.0 Hz, 1H), 8.28−8.36 (m, 1H). ^{13}C NMR (75.5 MHz, $CDCl_3$) δ 14.29, 22.77 (d, J = 5.0 Hz, 1C), 29.33, 29.83 (d, J = 19.7 Hz, 1C), 35.50, 47.24, 83.51 (d, J = 165.1 Hz, 1C), 105.97 (d, J = 3.9 Hz, 1C), 108.33, 108.61, 115.01 (d, J = 21.2 Hz, 1C), 117.97 (d, J = 5.8 Hz, 1C), 118.01, 124.03, 124.36 (d, J = 7.9 Hz, 1C), 124.50, 126.01, 126.33, 126.80, 126.82, 131.49, 132.21, 137.35 (d, J = 2.6 Hz, 1C), 139.76, 139.90, 141.66, 157.08 (d, J = 254.4 Hz, 1C), 190.54. HPLC 99% (Waters X-Bridge C-18 5 μm, 4.6 mm × 100 mm column, H_2O−CH_3CN, 35:65, UV detection at 254 nm). HRMS: Calculated for $C_{27}H_{28}NOF_2$ (M + H) 420.2139, found, 420.2151 (M + H).

*4-(2-Iodoethyl)morpholine (**1-5**, X = I).* 4-(2-Chloroethyl)-morpholine hydrochloride (5 g, 0.0269 mol) and sodium iodide (20 g, 0.1334 mol) were placed in acetone (50 mL) and refluxed for 16 h. Chloroform (50 mL) and brine solution (50 mL) were then added and the mixture stirred for 10 min. The solid was removed by filtration and added to a mixture of chloroform (50 mL) and saturated sodium bicarbonate solution (50 mL). The mixture was stirred for 5 min and the organic layer removed. The aqueous layer was then extracted with additional chloroform (2 × 25 mL). The organic layers were combined, washed with brine, and dried over sodium sulfate. The solvent was removed under reduced pressure to give the title product as a yellow oil (3.05 g, 47%), which contained approximately 5% 4-(2-chloroethyl)-morpholine. ^{1}H NMR (300 MHz, $CDCl_3$) δ 2.49 (t, J = 4.7 Hz, 4H), 2.72 (t, J = 7.6 Hz, 2H), 3.21 (t, J = 7.6 Hz, 2H), 3.71 (t, J = 4.7 Hz, 4H).

*4-[(1-Pentyl-1H-indol-3-yl)carbonyl]naphthalene-1-carboxylic Acid (**1-7a**).* Ethyl 4-[(1-pentyl-1*H*-indol-3-yl)carbonyl]naphthalene-1-carboxylate (**1-4c**) (3.0 g, 0.0073 mol) was dissolved in dioxane (50 mL). Sodium hydroxide solution (5N, 50 mL) was added and the mixture refluxed for 3 h. The solution was then allowed to cool to room temperature and stir overnight. The layers were separated and the solvent removed from the organic layer. The resulting residue was dissolved in water (50 mL) and extracted with EtOAc (2 × 50 mL) to remove unreacted starting material. The pH of the aqueous layer was then adjusted to 3 by the addition of HCl solution (1N) and extracted with EtOAc (2 × 50 mL). The organic layers were combined and dried over sodium sulfate. The solvent was removed under reduced pressure to give the title compound as a golden foam (2.05 g, 73%). ^{1}H NMR (300 MHz, $CDCl_3$) δ 0.85 (t, J = 6.7 Hz, 3H), 1.18−1.38 (m, 4H), 1.74−1.87 (m, 2H), 4.06 (t, J = 6.7 Hz, 2H), 7.31 (s, 1H), 7.34−7.45 (m, 3H), 7.48−7.57 (m, 1H), 7.63−7.72 (m, 2H), 8.17 (d, J = 8.4 Hz, 1H), 8.43 (d, J = 7.4 Hz, 1H), 8.45−8.53 (m, 1H), 9.11 (d, J = 8.7 Hz, 1H), OH proton not observed.

*N-Methyl-4-[(1-pentyl-1H-indol-3-yl)carbonyl]naphthalene-1-carboxamide (**1-7b**).* 4-[(1-Pentyl-1*H*-indol-3-yl)carbonyl]-naphthalene-1-carboxylic acid (**1-7a**) (830 mg, 2.15 mmol) was dissolved in THF (50 mL) and cooled in an ice bath. Oxalyl chloride (0.6 mL) was then added dropwise to the stirred solution under nitrogen. After the addition was complete (2 min), the mixture was stirred an additional 10 min at 0 °C and then at room temperature overnight. Subsequently, the solvent was removed under reduced pressure and the residue redissolved in THF (50 mL). The resulting solution was cooled to 0 °C in an ice bath, aqueous methylamine (1.5 mL, 40%) added, and the mixture stirred at 0 °C for 15 min. The ice bath was removed and the solution stirred at room temperature for 5 min. The solvent was removed under reduced pressure and the residue partitioned between EtOAc (75 mL) and water (75 mL). The organic layer was removed and the aqueous layer extracted with additional EtOAc (50 mL). The organic layers were combined, washed with brine, and dried over anhydrous sodium sulfate. The solvent was removed under reduced pressure and the residue purified over silica gel (Isco, gradient from 100% hexane to 60% EtOAc/40% hexane) to give the title compound as a golden foam (750 mg, 87%). ^{1}H NMR (300 MHz, $CDCl_3$) δ 0.83 (t, J = 6.8 Hz, 3H), 1.15−1.35 (m, 4H), 1.71−1.83 (m, 2H), 3.12 (d, J = 4.9 Hz, 3H), 4.03 (t, J = 7.1 Hz, 2H), 6.44−6.55 (m, 1H), 7.23 (s, 1H), 7.32−7.52 (m, 7H), 8.08 (d, J = 8.3 Hz, 1H), 8.26 (d, J = 8.6 Hz, 1H), 8.43−8.52 (m, 1H). ^{13}C NMR (75.5 MHz, $CDCl_3$) δ 13.84, 22.14, 26.90, 28.90, 29.40, 47.24, 110.10, 117.36, 122.82, 123.08, 123.61, 123.78, 124.08, 125.65, 126.23, 126.79, 127.06, 127.35, 130.36, 130.97, 136.20, 137.12, 138.44, 141.23, 170.08, 191.58. HPLC 98% (Waters X-Bridge C-18 5 μm, 4.6 mm × 100 mm column, 10 mM aqueous NH_4OAc−CH_3CN, 40:60, UV detection at 254 nm). HRMS: calculated for $C_{26}H_{27}N_2O_2$ (M + H) 399.2073, found 399.2069 (M + H).

*4-[(1-Pentyl-1H-indol-3-yl)carbonyl]naphthalene-1-carboxamide (**1-7c**).* Prepared as for **1-7b** with aqueous ammonium hydroxide (1.5 mL, 30%) and similarly chromatographed on silica gel (Isco, gradient from 100% hexane to 70% EtOAc/30% hexane) to give the title compound as a white solid (810 mg, 81%). ^{1}H NMR (300 MHz, $CDCl_3$) δ 0.83 (t, J = 6.6 Hz, 3H), 1.14−1.36 (m, 4H), 1.70−1.84 (m, 3H), 4.03 (t, J = 7.2 Hz, 2H), 6.27 (broad s, 1H), 6.47 (broad s, 1H), 7.25 (s, 1H), 7.31−7.61 (m, 6H), 7.68 (d, J = 7.2 Hz, 1H), 8.10 (d, J = 8.4 Hz, 1H), 8.38 (d, J = 8.3 Hz, 1H), 8.43−8.52 (m, 1H). ^{13}C NMR (75.5 MHz, $CDCl_3$) δ 13.84, 22.14, 28.89, 29.41, 47.26, 110.11, 117.34, 122.83, 123.12, 123.82, 123.99, 124.06, 125.63, 126.32, 126.78, 127.16, 127.56, 130.27, 131.04, 134.80, 137.13, 138.37, 141.75, 171.40, 191.43. HPLC 98% (Waters X-Bridge C-18 5 μm, 4.6 mm × 100 mm column, 10 mM aqueous NH_4OAc−CH_3CN, 40:60, UV detection at 254 nm). HRMS: calculated for $C_{25}H_{25}N_2O_2$ (M + H) 385.1916, found 385.1920 (M + H).

*1-{4-[(1-Pentyl-1H-indol-3-yl)carbonyl]naphthalen-1-yl}[34]propan-1-one (**1-7d**).* 4-[(1-Pentyl-1*H*-indol-3-yl)carbonyl]-naphthalene-1-carboxylic acid (**1-7a**) (830 mg, 2.15 mmol) was dissolved in THF (40 mL). DMF (0.2 mL) was added and the mixture purged with nitrogen. Oxalyl chloride (0.8 mL) was then added dropwise to the stirred solution over several minutes. After the addition was complete, the mixture was stirred at room temperature overnight. At the end of this time, the mixture was filtered to remove a small amount of solid material and the solvent removed from the filtrate under reduced pressure. The residue was dissolved in toluene (40 mL), and the resulting solution was cooled to 0 °C in a ice bath. Diethyl zinc (5.18 mL, 1 M in hexanes, 5.18 mmol) was then added over 2 min and the mixture stirred at 0 °C for an additional 10 min. The ice bath was removed and the solution stirred at room temperature for 4.5 h. The reaction was quenched with saturated ammonium chloride solution (40 mL total) and EtOAc (40 mL) was added. The mixture was stirred for 20 min, the organic layer removed, and the aqueous layer extracted with additional EtOAc (40 mL). The organic layers were combined, and the solvent was removed under reduced pressure. The reaction was repeated using 410 mg of **1-7a** (1.24 g total between the two reactions) and the material from both reactions combined. The residue was initially purified over silica gel (Isco, 120 g column, gradient from 100% hexane to 30% EtOAc/70% hexane) and subsequently twice by preparative thin layer chromatography (silica, 20 cm × 20 cm plate, 1000 μm, dichloromethane). A final purification by preparative thin layer chromatography (15% EtOAc/85% hexane) afforded the title compound as an off-white solid (two fractions: 11.6 mg, 98% pure by HPLC, 0.91%; 6.2 mg, 98% pure by HPLC, 0.48%). ^{1}H NMR (300 MHz, $CDCl_3$) δ 0.83 (t, J = 6.7 Hz, 3H), 1.19−1.37 (m, 4H), 1.32 (t, J = 7.2 Hz, 3H),1.73−1.86 (m, 2H), 3.12 (q, J = 7.3 Hz, 2H), 4.05 (t, J = 7.2 Hz, 2H), 7.28 (s, 1H), 7.32−7.43 (m, 3H), 7.44−7.53 (m, 1H), 7.54−7.66 (m, 2H), 7.82 (d, J = 7.3 Hz, 1H), 8.13 (d, J = 8.4 Hz, 1H), 8.42−8.52 (m, 2H). ^{13}C NMR (75.5 MHz, $CDCl_3$) δ 8.58, 13.83, 22.14, 28.91, 29.45, 35.91, 47.26, 110.06, 117.39, 122.91, 123.10, 123.70, 123.81, 125.15, 125.76, 126.43, 126.79. 127.08, 127.93, 130.30. 131.30, 137.12, 138.11, 138.21, 142.73. 191.29, 205.75. HPLC (Waters X-Bridge C-18 5 μm, 4.6 mm × 100 mm column, H_2O−CH_3CN, 35:65, UV detection at 254 nm). HRMS: calculated for $C_{27}H_{28}NO_2$ (M + H) 398.2120; found 398.2131 (M + H).

*4-[2-(1H-Inden-3-yl)ethyl]morpholine (**2-3**).* Indene (**2**−**1**) (10 g, 0.086 mol) was dissolved in anhydrous THF (130 mL) and the solution cooled in a dry ice/acetonitrile bath. nBuLi (0.0538 L, 1.6 M in hexane, 0.0861 mol) was then added dropwise over 10 min. The cooling was

DOI: 10.1021/acs.jmedchem.6b00516
J. Med. Chem. 2016, 59, 7525−7543

continued for 10 min, the bath removed, and the solution stirred at room temperature for 20 min. The mixture was again cooled in a dry ice/acetonitrile bath and 4-(2-chloroethyl)morpholine (**2-2**) (12.89 g, 0.0861 mmol) added dropwise over 10 min. The cooling was continued for 10 min, the bath removed, and the solution stirred overnight at room temperature. The mixture was quenched with methanol (20 mL) and the solvent removed under reduced pressure. The residue was partitioned between CH_2CL_2 (50 mL) and water (50 mL). The organic layer was removed and the aqueous layer extracted with additional CH_2Cl_2 (50 mL). The organic layers were combined, filtered through Celite, and the solvent removed under reduced pressure to give a crude mixture of (**1-yl**) and (**3-yl 2-3**). The residue was dissolved in dioxane (75 mL) and NaOH solution (4N, 75 mL) added to the mixture. The resulting solution was then heated under reflux for 5 h. Subsequently, the organic layer was removed and EtOAc (50 mL) and water (50 mL) added to the aqueous layer. The resulting mixture was shaken, the organic layer removed, and the aqueous layer extracted with additional EtOAc (2 × 25 mL). The organic layers were combined, washed with water, and dried over sodium sulfate. The solvent was removed under reduced pressure and residue was columned over silica gel (Isco, gradient from 100% hexane to 80% EtOAc/20% hexane) to give recovered indene (890 mg) and the title product (**2-3**) as a yellow oil (8.92 g, 45%). ^{1}H NMR (300 MHz, $CDCl_3$) δ 2.56 (t, J = 4.6 Hz, 4H), 2.66−2.83 (m, 4H), 3.33 (d, J = 4.7 Hz, 2H), 3.77 (t, J = 4.7 Hz, 4H), 6.26 (s, 1H), 7.17−7.24 (m, 1H), 7.26−7.34 (m, 1H), 7.35−7.41 (m, 1H), 7.46 (d, J = 7.3 Hz, 1H).

*4-Ethylnaphthalene-1-carbaldehyde (**2-4t**).* Prepared as for **2-4u** in 51% yield. Light-brown oil. ^{1}H NMR (300 MHz, $CDCl_3$) δ 1.41 (t, J = 7.5 Hz, 3H), 3.18 (q, J = 7.5 Hz, 2H), 7.50 (d, J = 7.3 Hz, 1H), 7.55−7.70 (m, 2H), 7.90 (d, J = 7.3 Hz, 1H), 8.13 (d, J = 8.5 Hz, 1H), 9.33 (d, J = 8.4 Hz, 1H), 10.33 (s, 1H).

*4-Propylnaphthalene-1-carbaldehyde (**2-4u**).* Dichloromethyl methyl ether (0.39 mL, 97%, 4.2 mmol) was dissolved in dichloroethane (5 mL) and cooled to 0 °C. $TiCl_4$ (0.46 mL, 4.2 mmol) was added dropwise over 2 min. Once the addition was complete, the solution was stirred at 0 °C for 45 min. 1-Propyl naphthalene (550 mg, 3.23 mmol) in dichloroethane (5 mL) was then added dropwise over 5 min. The solution was allowed to warm to room temperature and stirred overnight. The reaction mixture was then poured into ice−water (100 mL), the organic layer removed, and the aqueous layer extracted with dichloroethane (2 × 25 mL). The organic layers were combined, washed with saturated sodium bicarbonate solution and water, and dried over sodium sulfate. The solvent was removed under reduced pressure, and the residue was columned over silica gel (Isco, gradient from 100% hexane to 10% EtOAc/90% hexane) to give the title product as a light-brown oil (480 mg, 75%). ^{1}H NMR (300 MHz, $CDCl_3$) δ 1.05 (t, J = 7.4 Hz, 3H), 1.74−1.88 (m, 2H), 3.11 (t, J = 7.5 Hz, 2H), 7.47 (d, J = 7.3 Hz, 1H), 7.57−7.71 (m, 2H), 7.89 (d, J = 7.3 Hz, 1H), 8.09−8.16 (m, 1H), 9.30−9.37 (m, 1H), 10.33 (s, 1H).

*4-{2-[(1E)-1-(Arylidene)-1H-inden-3-yl]ethyl}morpholine (**2-5a−2-5u**).* Method 1 (**2-5a−e**): Reflux 18 h or Method 2 (**2-5f−u**): Microwave for 15−17 min; with variations in purification of the reaction residue after cooling and evaporation that were either recrystallization or silica gel chromatography typified by preparation of **2-5d** (method 1) or **2-5h** (method 2).

*4-{2-[(1E)-1-[(2-Fluorophenyl)methylidene]-1H-inden-3-yl]ethyl}-morpholine (**2-5d**): Method 1.* Method 1: 4-[2-(1*H*-Inden-3-yl)ethyl]-morpholine (**2-3**) (260 mg, 1.13 mmol) was dissolved in methanol (1.0 mL) and the reaction mixture purged with nitrogen. Sodium methoxide (2.50 mL, 0.5 M in MeOH; 1.25 mmol) was added dropwise over 5 min, and the solution stirred for 10 min. 2-Fluorobenzaldehyde (0.14 mL, 97%, 1.29 mmol) was added dropwise and the mixture stirred for 5 min. The solution was then heated under reflux for 18 h then allowed to cool to room temperature, and the solvent was removed under reduced pressure. The residue was purified over silica gel (Isco, 120 g column, 100% EtOAc) to give the title compound as a yellow film (76 mg, 93% pure by HPLC, 20%). A second fraction of less pure material was also collected (42 mg, 91% pure by HPLC, 11%). ^{1}H NMR (300 MHz, $CDCl_3$) δ 2.56 (t, J = 4.6 Hz, 4H), 2.68−2.77 (m, 2H), 2.79−2.90 (m, 2H), 3.76 (t, J = 4.7 Hz, 4H), 6.72 (s, 1H), 7.04−7.43 (m, 6H), 7.48 (s, 1H), 7.58−7.74 38 (m, 2H). ^{13}C NMR (75.5 MHz, $CDCl_3$) δ 25.46, 53.75 (2C), 57.49, 67.07 (2C), 115.72 (d, J = 21.9 Hz, 1C), 118.50 (d, J = 4.6 Hz, 1C), 118.74, 119.38, 121.91, 124.16 (d, J = 3.6 Hz, 1C) 125.21 (d, J = 13.4 Hz, 1C), 125.62, 127.70, 129.77 (d, J = 8.4 Hz, 1C), 131.66 (d, J = 2.8 Hz, 1C), 137.90, 140.84, 142.43, 147.25, 161.09 (d, J = 250.1 Hz, 1C). HPLC (Waters X-Bridge C-18 5 μm, 4.6 mm × 100 mm column, 10 mM aqueous NH_4OAc−CH_3CN, 40:60, UV detection at 254 nm). HRMS: calculated for $C_{22}H_{23}NOF$ (M + H) 336.1764, found 336.1763 (M + H).

*4-{2-[(1E)-1-(Naphthalen-1-ylmethylidene)-1H-inden-3-yl]ethyl}-morpholine (**2-5a**).* Golden solid (2.98 g, 66%). ^{1}H NMR (300 MHz, $CDCl_3$) δ 2.41 (t, J = 4.2 Hz, 4H), 2.54−2.64 (m, 2H), 2.71−2.82 (m, 2H), 3.56 (t, J = 4.5 Hz, 4H), 3H), 6.67 (s, 1H), 7.26−7.41 (m, 3H), 7.55−7.71 (m, 4H), 7.93−8.08 (m, 3H), 8.22−8.31 (m, 2H). ^{13}C NMR (75.5 MHz, $CDCl_3$) δ 24.65, 53.15 (2C), 56.74, 66.20 (2C), 118.76, 119.86, 122.11, 124.44, 124.52, 125.32, 125.65, 126.22, 126.55, 127.54, 128.47, 128.51, 128.87, 131.58, 133.21, 133.54, 137.31, 140.67, 142.28, 146.74. HPLC 99% (Waters X-Bridge C-18 5 μm, 4.6 mm × 100 mm column, 10 mM aqueous NH_4OAc−CH_3CN, 40:60, UV detection at 254 nm). HRMS: calculated for $C_{26}H_{26}NO$ (M + H) 368.2014, found 368.2013 (M + H).

*4-{2-[(1E)-1-(Phenylmethylidene)-1H-inden-3-yl]ethyl}-morpholine (**2-5b**).* Dark-yellow resin (258 mg, 46%). ^{1}H NMR (300 MHz, $CDCl_3$) δ 2.57 (t, J = 4.5 Hz, 4H), 2.70−2.79 (m, 2H), 2.81−2.91(m, 2H), 3.77 (t, J = 4.7 Hz, 4H, 6.83 (s, 1H), 7.21−7.48 (m, 7H), 7.56−7.63 (m, 2H), 7.66−7.72 (m, 1H). ^{13}C NMR (75.5 MHz, $CDCl_3$) δ 25.42, 53.75 (2C), 57.57, 67.05 (2C), 118.71, 119.04, 122.06, 125.41, 126.62, 127.39, 128.09, 128.68 (2C), 130.10 (2C), 137.23, 138.24, 139.41, 142.23, 146.58. HPLC 99% (Waters X-Bridge C-18 5 μm, 4.6 mm × 100 mm column, 10 mM aqueous ammonium formate−acetonitrile, 40:60, UV detection at 254 nm). HRMS: calculated for $C_{22}H_{24}NO$ (M + H) 318.1858, found 318.1857 (M + H).

*4-{2-[(1E)-1-[(2-Iodophenyl)methylidene]-1H-inden-3-yl]ethyl}-morpholine (**2-5c**).* Yellow solid (1.00 g, 57%). ^{1}H NMR (300 MHz, $CDCl_3$) δ 2.55 (t, J = 4.6 Hz, 4H), 2.66−2.75 (m, 2H), 2.77−2.87 (m, 2H), 3.75 (t, J = 4.6 Hz, 4H), 3H), 6.57 (s, 1H), 6.98−7.07 (m, 1H), 7.22−7.34 (m, 3H), 7.35−7.47 (m, 2H), 7.52−7.59 (m, 1H), 7.71−7.79 (m, 1H), 7.89−7.97 (m, 1H). ^{13}C NMR (75.5 MHz, $CDCl_3$) δ 25.45, 53.74 (2C), 57.43, 67.06 (2C), 100.92, 118.80, 119.49, 121.87, 125.63, 127.83, 128.12, 129.26, 129.92, 131.65, 137.57, 139.35, 140.52, 140.54, 142.64, 147.05. HPLC 98% (Waters X-Bridge C-18 5 μm, 4.6 mm × 100 mm column, 10 mM aqueous NH_4OAc−CH_3CN, 40:60, UV detection at 254 nm). HRMS: calculated for $C_{22}H_{23}NOI$ (M + H) 444.0824, found 444.0828 (M + H).

*4-{2-[(1E)-1-[(3-Phenylphenyl)methylidene]-1H-inden-3-yl]ethyl}-morpholine (**2-5e**).* Yellow film (21%). ^{1}H NMR (300 MHz, $CDCl_3$) δ 2.56 (t, J = 4.4 Hz, 4H), 2.69−2.79 (m, 2H), 2.80−2.91 (m, 2H), 3.74 (t, J = 4.6 Hz, 4H), 6.87 (s, 1H), 7.21−7.34 (m, 3H), 7.35−7.73 (m, 10H), 7.79 (s, 1H). ^{13}C NMR (75.5 MHz, $CDCl_3$) δ 25.42, 53.72 (2C), 57.56, 67.03 (2C), 118.78, 119.11, 122.14, 125.48, 126.50, 126.97, 127.23 (2C), 127.48, 127.59, 128.90 (4C), 129.12, 137.73, 138.24, 139.75, 140.90, 141.78, 142.29, 146.80. HPLC 94% (Waters X-Bridge C-18 5 mm, 4.6 mm × 100 mm column, 10 mM aqueous NH_4OAc−CH_3CN, 35:65, UV detection at 254 nm). HRMS: calculated for $C_{28}H_{28}NO$ (M + H) 394.2171; found 394.2176 (M + H).

*4-{2-[(1E)-1-[(2-Methoxyphenyl)methylidene]-1H-inden-3-yl]-ethyl}morpholine (**2-5h**): Methods 2.* Method 2: 4-[2-(1*H*-Inden-3-yl)ethyl]morpholine (**2-3**) (260 mg, 1.13 mmol) and methanol (1.5 mL) were placed in a 10 mL microwave tube equipped with a rubber septa. The system was purged with nitrogen, sodium methoxide (2.30 mL, 0.5 M in MeOH; 1.15 mmol) added dropwise over 5 min and the solution stirred for 10 min. 2-Methoxybenzaldehyde (0.15 mL, 98%, 1.22 mmol) was added and the mixture stirred for an additional 5 min. The septa was replaced with a microwave cap and the tube irradiated for 15.0 min at 105 °C. Subsequently, the mixture was allowed to cool to room temperature and the solvent removed under reduced pressure. The residue was purified over silica gel (Isco, 120 g column, 100% EtOAc) to give two fractions of title compound (13 mg, 96% pure by HPLC, 3.3%; 110 mg, 95% pure by HPLC, 28%). ^{1}H NMR (300 MHz, $CDCl_3$) δ 2.56 (t, J = 4.5 Hz, 4H), 2.68−2.78 (m, 2H), 2.80−2.90 (m,

DOI: 10.1021/acs.jmedchem.6b00516
J. Med. Chem. 2016, 59, 7525−7543

2H), 3.76 (t, J = 4.6 Hz, 4H), 3.90 (s, 3H), 6.75 (s, 1H), 6.94 (d, J = 8.2 Hz, 7.04 (t, J = 5.0 Hz, 1H), 7.18−7.38 (m, 4H), 7.55−7.62 (m, 1H), 7.67 (s,1H), 7.71−7.78 (d, J = 6.7 Hz, 1H). ^{13}C NMR (75.5 MHz, $CDCl_3$) δ 25.42, 53.76 (2C), 55.59, 57.53, 67.08 (2C), 110.69, 118.53, 119.33, 120.61, 122.38 (2C), 126.36, 127.14, 129.60, 130.19, 131.75, 138.19, 139.18, 142.37, 145.82, 158.20. HPLC (Waters X-Bridge C-18 5 μm, 4.6 mm × 100 mm column, 10 mM aqueous NH_4OAc-CH_3CN, 40:60, UV detection at 254 nm). HRMS: calculated for $C_{23}H_{25}NO_2$ (M + H) 348.1964, found 348.1967 (M + H).

*4-{2-[(1E)-1-[(2-Chlorophenyl)methylidene]-1H-inden-3-yl]ethyl}-morpholine (**2-5f**).* Yield 85 mg, 97% pure by HPLC, 20%. ^{1}H NMR (300 MHz, $CDCl_3$) δ 2.55 (t, J = 4.5 Hz, 4H), 2.66−2.76 (m, 2H), 2.78−2.88 (m, 2H), 3.75 (t, J = 4.7 Hz, 4H), 3H), 6.63 (s, 1H), 7.22−7.37 (m, 5H), 7.42−7.48 (m, 1H), 7.55−7.64 (m,2H), 7.71−7.77 (m, 1H). ^{13}C NMR (75.5 MHz, $CDCl_3$) δ 25.44, 53.74 (2C), 57.46, 67.06 (2C), 118.77, 119.51, 121.85, 123.09, 125.63, 126.70, 127.82, 129.12, 129.74, 132.21, 134.77, 135.48, 137.72, 140.96, 142.60, 147.29. HPLC (Waters X-Bridge C-18 5 μm, 4.6 mm × 100 mm column, 10 mM aqueous NH_4OAc−CH_3CN, 40:60, UV detection at 254 nm). HRMS: calculated for $C_{22}H_{23}NOCl$ (M + H) 352.1468, found 352.1455 (M + H).

*4-{2-[(1E)-1-[(2-Bromophenyl)methylidene]-1H-inden-3-yl]ethyl}-morpholine (**2-5g**).* Yield 157 mg, 95% pure by HPLC, 34%. ^{1}H NMR (300 MHz, $CDCl_3$) δ 2.54 (t, J = 4.4 Hz, 4H), 2.65−2.75 (m, 2H), 2.76−2.87 (m, 2H), 3.75 (t, J = 4.7 Hz, 4H), 3H), 6.60 (s, 1H), 7.14−7.42 (m, 5H), 7.50 (s, 1H), 7.55−7.67 (m, 2H), 7.70−7.76 (m, 1H). ^{13}C NMR (75.5 MHz, $CDCl_3$) δ 25.44, 53.74 (2C), 57.44, 67.06 (2C), 118.77, 119.51, 121.85, 125.08, 125.48, 125.63, 127.29, 127.82, 129.26, 132.33, 132.93, 137.21, 137.66, 140.81, 142.620, 147.21. HPLC (Waters X-Bridge C-18 5 μm, 4.6 mm × 100 mm column, 10 mM aqueous NH_4OAc−CH_3CN, 40:60, UV detection at 254 nm). HRMS: calculated for $C_{22}H_{23}NOBr$ (M + H) 396.0963, found 396.0959 (M + H).

*4-{2-[(1E)-1-[(2-Methylphenyl)methylidene]-1H-inden-3-yl]ethyl}-morpholine (**2-5i**).* Yield 251 mg, 94% pure by HPLC, 63%. ^{1}H NMR (300 MHz, $CDCl_3$) δ 2.42 (s, 3H), 2.55 (t, J = 4.2 Hz, 4H), 2.67−2.76 (m, 2H), 2.79−2.89 (m, 2H), 3.76 (t, J = 4.6 Hz, 4H), 6.64 (s, 1H), 7.20−7.36 (m, 6H), 7.45−7.54 (m, 2H), 7.73 (d, J = 6.7 Hz, 1H). ^{13}C NMR (75.5 MHz, $CDCl_3$) δ 20.13, 25.38, 53.75 (2C), 57.53, 67.06 (2C), 118.68, 119.13, 122.56, 125.30, 125.41, 125.88, 127.45, 128.14, 130.19, 130.94, 136.19, 137.44, 137.78, 139.93, 142.65, 146.01. HPLC (Waters X-Bridge C-18 5 μm, 4.6 mm × 100 mm column, 10 mM aqueous NH_4OAc−CH_3CN, 40:60, UV detection at 254 nm). HRMS: calculated for $C_{23}H_{26}NO$ (M + H) 332.2014, found 332.2022 (M + H).

*4-{2-[(1E)-1-[(4-Methoxynaphthalen-1-yl)methylidene]-1H-inden-3-yl]ethyl}morpholine (**2-5j**).* Yellow solid (134 mg, 31%). ^{1}H NMR (300 MHz, $CDCl_3$) δ 2.51 (t, J = 4.5 Hz, 4H), 2.64−2.75 (m, 2H), 2.77−2.87 (m, 2H), 3.73 (t, J = 4.6 Hz, 4H), 4.02 (s, 3H), 6.67 (s, 1H), 6.87 (d, J = 8.0 Hz, 1H), 7.25−7.38 (m, 3H), 7.46−7.61 (m, 3H), 7.75−7.84 (m, 1H), 7.96 (s, 1H), 8.04−8.12 (m, 1H), 8.29−8.38 (m, 1H). ^{13}C NMR (75.5 MHz, $CDCl_3$) δ 25.41, 53.76 (2C), 56.66, 57.61, 67.07 (2C), 103.76, 118.71, 119.17, 122.62, 122.95, 124.42, 124.61, 125.27, 125.53, 125.67, 126.61, 127.06, 127.29, 129.79, 133.15, 137.84, 139.99, 142.77, 145.42, 156.05. HPLC 95% (Waters X-Bridge C-18 5 μm, 4.6 mm × 100 mm column, 10 mM aqueous ammonium formate−acetonitrile, 40:60, UV detection at 254 nm). HRMS: calculated for $C_{27}H_{28}NO_2$ (M + H) 398.2120, found 398.2124 (M + H).

*4-{2-[(1E)-1-[(2-Phenylphenyl)methylidene]-1H-inden-3-yl]ethyl}-morpholine (**2-5k**).* Yellow film (133 mg, 30%). ^{1}H NMR (300 MHz, $CDCl_3$) δ 2.56 (t, J = 4.4 Hz, 4H), 2.69−2.80 (m, 2H), 2.81−2.92 (m, 2H), 3.76 (t, J = 4.6 Hz, 4H), 6.84 (s, 1H), 7.09−7.18 (m, 1H), 7.22−7.48 (m, 12H), 7.64−7.73 (m, 1H). ^{13}C NMR (75.5 MHz, $CDCl_3$) δ 25.51, 53.84 (2C), 57.66, 67.12 (2C), 118.66, 119.33, 122.56, 125.34, 127.03, 127.36, 127.38, 127.47, 128.23 (2C), 128.33, 130.02 (2C), 130.12, 131.94, 135.20, 137.94, 139.45, 140.62, 142.42, 146.46, 146.09. HPLC 92% (Waters X-Bridge C-18 5 μm, 4.6 mm × 100 mm column, 10 mM aqueous NH_4OAc−CH_3CN, 35:65, UV detection at 254 nm). HRMS: calculated for $C_{28}H_{28}NO$ (M + H) 394.2171, round 394.2176 (M + H).

*7-{[(1E)-3-[2-(Morpholin-4-yl)ethyl]-1H-inden-1-ylidene]methyl}-1H-indole (**2-5l**).* Yellow film (115 mg, 31%). ^{1}H NMR (300 MHz, $CDCl_3$) δ 2.49 (t, J = 4.4 Hz, 4H), 2.60−2.72 (m, 2H), 2.73−2.86 (m, 2H), 3.72 (t, J = 4.5 Hz, 4H), 6.55−6.65 (m, 1H), 6.67 (s, 1H), 7.12−7.40 (m, 6H), 7.57 (s, 1H), 7.60−7.78 (m, 2H), 8.63 (s, 1H). ^{13}C NMR (75.5 MHz, $CDCl_3$) δ 25.34, 53.71 (2C), 57.46, 67.04 (2C), 103.17, 118.95, 119.20, 120.18, 120.94, 121.32, 122.30, 122.73, 124.14, 124.42, 125.55, 127.56, 128.47, 134.55, 137.81, 140.22, 142.61, 146.31. HPLC 94% (Waters X-Bridge C-18 5 μm, 4.6 mm × 100 mm column, 10 mM aqueous NH_4OAc−CH_3CN, 35:65, UV detection at 254 nm). HRMS: calculated for $C_{24}H_{25}N_2O$ (M + H) 357.1967, found 357.1966 (M + H).

*4-{2-[(1E)-1-(Thiophen-2-ylmethylidene)-1H-inden-3-yl]ethyl}-morpholine (**2-5m**).* Yellow solid (235 mg, 67%). ^{1}H NMR (300 MHz, $CDCl_3$) δ 2.56 (t, J = 4.5 Hz, 4H), 2.68−2.78 (m, 2H), 2.80−2.90 (m, 2H), 3.76 (t, J = 4.6 Hz, 4H), 7.01 (s, 1H), 7.03−7.09 (m, 1H), 7.16−7.31 (m, 4H), 7.37−7.44 (m, 2H), 7.55−7.64 (m, 2H). ^{13}C NMR (75.5 MHz, $CDCl_3$) δ 25.47, 53.77 (2C), 57.56, 67.10 (2C), 118.90, 118.97 (2C), 121.85, 125.40, 127.11, 127.64, 128.53, 131.03, 136.79, 138.39, 140.96, 142.14, 146.37. HPLC 94% (Waters X-Bridge C-18 5 μm, 4.6 mm × 100 mm column, 10 mM aqueous NH_4OAc−CH_3CN, 35:65, UV detection at 254 nm). HRMS: calculated for $C_{20}H_{22}NOS$ (M + H) 324.1422, found 324.1431 (M + H).

*4-{2-[(1E)-1-(Furan-2-ylmethylidene)-1H-inden-3-yl]ethyl}-morpholine (**2-5n**).* Yellow solid (231 mg, 64%). ^{1}H NMR (300 MHz, $CDCl_3$) δ 2.47−2.53 (m, 4H), 2.70−2.96 (m, 4H), 3.65−3.90 (m, 4H), 6.45−6.55 (m, 1H), 6.57−6.65 (m, 1H), 6.98 (s, 1H), 7.10−7.34 (m, 4H), 7.50−7.64 (m, 2H). ^{13}C NMR (75.5 MHz, $CDCl_3$) δ 25.48, 53.79 (2C), 57.67, 67.08 (2C), 112.26, 112.38, 114.22, 118.81, 118.88, 123.24, 125.18, 127.13, 136.02, 138.19, 142.17, 144.38, 145.68, 153.52. HPLC 94% (Waters X-Bridge C-18 5 μm, 4.6 mm × 100 mm column, 10 mM aqueous NH_4OAc−CH_3CN, 40:60, UV detection at 254 nm). HRMS: calculated for $C_{20}H_{22}NO_2$ (M + H) 308.1651, found 308.1632 (M + H).

*5-{[(1E)-3-[2-(Morpholin-4-yl)ethyl]-1H-inden-1-ylidene]methyl}-isoquinoline (**2-5o**).* Yellow solid (70 mg, 17%, 93% pure by HPLC). ^{1}H NMR (300 MHz, $CDCl_3$) δ 2.53 (t, J = 4.5 Hz, 4H), 2.65−2.75 (m, 2H), 2.77−2.88 (m, 2H), 3.74 (t, J = 4.5 Hz, 4H), 6.56 (s, 1H), 7.27−7.40 (m, 3H), 7.62−7.72 (m, 1H), 7.76−7.94 (m, 4H), 7.98 (d, J = 8.1 Hz, 1H), 8.58 (d, J = 5.9 Hz, 1H), 9.30 (s, 1H). ^{13}C NMR (75.5 MHz, $CDCl_3$) δ 25.43, 53.72 (2C), 57.40, 67.03 (2C), 117.53, 118.93, 119.39, 121.97, 122.23, 125.69, 126.88, 127.84, 128.01, 128.78, 132.68, 133.45, 134.84, 137.41, 142.37, 142.89, 143.65, 147.35, 153.09. HPLC (Waters X-Bridge C-18 5 μm, 4.6 mm × 100 mm column, 10 mM aqueous ammonium formate−acetonitrile, 40:60, UV detection at 254 nm). HRMS: calculated for $C_{25}H_{25}N_2O$ (M + H) 369.1967; found 369.1961 (M + H).

*4-{[(1E)-3-[2-(Morpholin-4-yl)ethyl]-1H-inden-1-ylidene]methyl}-quinoline (**2-5p**).* Yellow solid (25 mg, 5.8%). ^{1}H NMR (300 MHz, $CDCl_3$) δ 2.55 (t, J = 4.4 Hz, 4H), 2.65−2.76 (m, 2H), 2.78−2.89 (m, 2H), 3.75 (t, J = 4.5 Hz, 4H), 6.54 (s, 1H), 7.27−7.40 (m, 3H), 7.47 (d, J = 4.4 Hz, 1H), 7.55−7.64 (m, 1H), 7.70−7.82 (m, 2H), 7.85 (s, 1H), 8.02−8.22 (m, 2H) 8.97 (d, J = 4.4 Hz, 1H). ^{13}C NMR (75.5 MHz, $CDCl_3$) δ 25.34, 53.66 (2C), 57.24, 66.92 (2C), 119.06, 119.61, 120.86, 122.04, 122.51, 124.60, 125.93, 126.86, 127.20, 128.40, 129.59, 130.14, 137.12, 142.63, 143.06, 143.91, 148.17, 148.51, 149.93. HPLC 95% (Waters X-Bridge C-18 5 μm, 4.6 mm × 100 mm column, 10 mM aqueous NH_4OAc−CH_3CN, 40:60, UV detection at 254 nm). HRMS: calculated for $C_{25}H_{25}N_2O$ (M + H) 369.1967, found 369.1957 (M + H).

*4-{2-[(1E)-1-(1,2-Dihydroacenaphthylen-5-ylmethylidene)-1H-inden-3-yl]ethyl}morpholine (**2-5q**).* Yellow solid (120 mg, 26%). ^{1}H NMR (300 MHz, $CDCl_3$) δ 2.52 (t, J = 4.5 Hz, 4H), 2.65−2.75 (m, 2H), 2.77−2.87 (m, 2H), 3.41 (s, 4H), 3.74 (t, J = 4.5 Hz, 4H), 6.73 (s, 1H), 7.23−7.38 (m, 5H), 7.46−7.54 (m, 1H), 7.66 (d, J = 7.2 Hz, 1H), 7.76−7.86 (m, 2H), 7.96 (s, 1H). ^{13}C NMR (75.5 MHz, $CDCl_3$) δ 23.15, 28.04, 28.33, 51.49 (2C), 55.33, 64.81 (2C), 116.45, 116.53, 117.00, 117.52, 120.71, 121.61, 123.03, 125.06, 126.13, 127.82, 128.40, 128.53, 135.72, 137.16, 137.89, 139.83, 140.40, 143.46, 144.22, 144.64. HPLC 95% (Waters X-Bridge C-18 5 μm, 4.6 mm × 100 mm column, 10 mM aqueous NH_4OAc−CH_3CN, 40:60, UV detection at 254 nm). HRMS: calculated for $C_{28}H_{28}NO$ (M + H) 394.2171, found 394.2172 (M + H).

*4-{2-[(1E)-1-(Naphthalen-2-ylmethylidene)-1H-inden-3-yl]ethyl}-morpholine (**2-5r**).* Yellow film (172 mg, 38%). ^{1}H NMR (300 MHz, $CDCl_3$) δ 2.57 (t, J = 4.4 Hz, 4H), 2.70−2.80 (m, 2H), 2.81−2.93 (m, 2H), 3.77 (t, J = 4.6 Hz, 4H), 6.94 (s, 1H), 7.22−7.36 (m, 3H), 7.47−7.56 (m, 3H), 7.69−7.79 (m, 3H), 7.80−7.92 (m, 3H), 8.02 (s, 1H). ^{13}C

DOI: 10.1021/acs.jmedchem.6b00516
J. Med. Chem. 2016, 59, 7525−7543

NMR (75.5 MHz, $CDCl_3$) δ 23.35, 51.62 (2C), 55.46, 64.95 (2C), 116.63, 116.96, 120.02, 123.32, 124.39, 124.49, 124.55, 125.26, 125.29, 125.60, 126.14, 126.18, 127.76, 130.82, 131.38, 132.67, 136.19, 137.51, 140.05, 144.68. HPLC 99% (Waters X-Bridge C-18 5 μm, 4.6 mm × 100 mm column, 0.05% aqueous TFA−CH_3CN, 40:60, UV detection at 254 nm). HRMS: calculated for $C_{26}H_{26}NO$ (M + H) 368.2014, found 368.2011 (M + H).

*4-{2-[(1E)-1-(Phenanthren-4-ylmethylidene)-1H-inden-3-yl]-ethyl}morpholine (**2-5s**).* Yellow solid (190 mg, 37%). ^{1}H NMR (300 MHz, $CDCl_3$) δ 2.51 (t, J = 4.4 Hz, 4H), 2.64−2.73 (m, 2H), 2.78−2.88 (m, 2H), 3.73 (t, J = 4.6 Hz, 4H), 6.66 (s, 1H), 7.27−7.38 (m, 3H), 7.59−7.74 (m, 4H), 7.81−7.87 (m, 2H), 7.91−7.96 (m, 1H), 7.98 (m, 3H), 8.12−8.19 (m, 1H), 8.66−8.78 (m, 2H). ^{13}C NMR (75.5 MHz, $CDCl_3$) δ 25.41, 53.73 (2C), 57.45, 67.06 (2C), 118.83, 119.37, 122.67, 122.83, 123.13, 124.66, 125.47, 125.63, 126.85, 126.89, 126.98, 127.12, 127.71, 129.01, 130.05, 130.39, 130.44, 131.28, 131.57, 132.94, 137.51, 141.78, 143.13, 146.14. HPLC 99% (Waters X-Bridge C-18 5 μm, 4.6 mm × 100 mm column, 0.05% aqueous TFA−CH_3CN, 40:60, UV detection at 254 nm). HRMS: calculated for $C_{30}H_{28}NO$ (M + H) 418.2171, found 418.2174 (M + H).

*4-{2-[(1E)-1-[(4-Ethylnaphthalen-1-yl)methylidene]-1H-indenyl]-ethyl}morpholine (**2-5t**).* Yellow film (290 mg, 62%). ^{1}H NMR (300 MHz, $CDCl_3$) δ 1.40 (t, J = 7.6 Hz, 3H), 2.48 (t, J = 4.4 Hz, 4H), 2.60−2.70 (m, 2H), 2.73−2.85 (m, 2H), 3.12 (q, J = 7.5 Hz, 2H), 3.71 (t, J = 4.5 Hz, 4H), 6.63 (s, 1H), 7.22−7.34 (m, 3H), 7.38 (d, J = 7.4 Hz, 1H), 7.46−7.58 (m, 3H), 7.74−7.81 (m, 1H), 7.98 (s, 1H), 8.04−8.18 (m, 2H). ^{13}C NMR (75.5 MHz, $CDCl_3$) δ 15.08, 25.44, 26.14, 53.78 (2C), 57.58, 67.09 (2C), 118.79, 119.33, 123.02, 124.38, 124.68, 124.86, 125.41, 125.54, 126.03 (2C), 127.55, 129.19, 131.97, 132.55, 132.60, 137.77, 140.95, 141.18, 142.94, 145.89. HPLC 97% (Waters X-Bridge C-18 5 μm, 4.6 mm × 100 mm column, 10 mM aqueous NH_4OAc−CH_3CN, 40:60, UV detection at 254 nm). HRMS: calculated for $C_{28}H_{30}NO$ (M + H) 396.2327, found 396.2332 (M + H).

*4-{2-[(1E)-1-[(4-Propylnaphthalen-1-yl)methylidene]-1H-inden-3-yl]ethyl}morpholine (**2-5u**).* Yellow solid (135 mg, 96% pure by HPLC, 29%; scale up 913 mg, 62%). ^{1}H NMR (300 MHz, $CDCl_3$) δ 1.07 (t, J = 7.3 Hz, 3H), 1.74−1.90 (m, 2H), 2.53 (t, J = 4.5 Hz, 4H), 2.63−2.76 (m, 2H), 2.77−2.89 (m, 2H), 3.09 (q, J = 7.5 Hz, 2H), 3.74 (t, J = 4.6 Hz, 4H), 6.65 (s, 1H), 7.25−7.36 (m, 3H), 7.39 (d, J = 7.3 Hz, 1H), 7.48−7.60 (m, 3H), 7.77−7.84 (m, 1H), 8.00 (s, 1H), 8.07−8.19 (m, 2H). ^{13}C NMR (75.5 MHz, $CDCl_3$) δ 14.36, 23.97, 25.40, 35.38, 53.75 (2C), 57.55, 67.07 (2C), 118.73, 119.24, 123.00, 124.53, 124.83, 125.33, 125.46, 125.70, 125.90, 125.93, 127.48, 128.96, 132.08, 132.52, 132.60, 137.71, 139.67, 140.86, 142.89, 145.82. HPLC (Waters X-Bridge C-18 5 μm, 4.6 mm × 100 mm column, 10 mM aqueous ammonium formate−acetonitrile, 40:60, UV detection at 254 nm). HRMS: calculated for $C_{29}H_{32}NO$ (M + H) 410.2484, found 410.2474 (M + H).

CB1/CB2R Binding Assays. Detailed radioligand displacement assays (using the well-characterized CBR agonist (−)-*cis*-3-[2-hydroxy-4-(1,1-dimethylheptyl)phenyl]-*trans*-4-(3-hydroxypropyl)cyclohexanol [2,3,4-^{3}H] [^{3}H]-CP55940 as the radioligand)[42] were conducted to determine the affinity (K_i) of the test compounds for CB1R and CB2R as has been previously described by our group.[27,43] Heterologous competition binding assays were performed to calculate receptor affinities. Unlabeled **2**[26] or **3** were used as appropriate controls for nonspecific binding in the assay. Calculation of the equilibrium dissociation constant (K_i) was performed using the Cheng−Prusoff equation.

Calcium Flux Assay. Chinese hamster ovary cells stably expressing either human CB1 or CB2 cDNA and the promiscuous G-protein $G\alpha q_{16}$ were removed from their flasks using the nonenzymatic cell-stripper (Mediatech Inc.) and quenched with DMEM/F12, 10% FBS, centrifuged, and resuspended in the serum-containing media. Cells were counted with a hemocytometer and 40000 cells were transferred to each well of a black Costar 96-well optical bottom plate (Corning Corporation). Each plate was incubated at 37 °C for 24 h to confluence. The culture media were removed from the plates, and cells were subsequently loaded with a fluorescent calcium probe (Fluo-4 AM dye, Invitrogen/Molecular Probes) at a final loading concentration of 2 μM in a HBSS-based buffer containing 20 mM HEPES, 1% BSA, and 10 μM Probenecid (Sigma) in a total volume of 225 μL. Cells were incubated at 37 °C for 1 h and then stimulated with various concentrations of a test agent using a FlexStation plate-reader, which automatically added the agonist at 10× concentration to each well after reading baseline values for ∼17 s. Agonist-mediated change in fluorescence (488 nm excitation, 525 nm emission) was monitored in each well at 1 s intervals for 60 s and reported for each well. Data were collected using Softmax version 4.8 (MDS Analytical Technologies) and analyzed using Prism software (GraphPad). Nonlinear regression analysis was performed to fit data and obtain maximum response (E_{max}), effective concentration for 50% response (EC_{50}), correlation coefficient (r^2), and other parameters. All experiments were performed 3−6 times to ensure reproducibility and data reported as mean ± standard error of the mean unless noted otherwise.

MDCK-mdr1 Permeability Assays. MDCK-mdr1 cells obtained from The Netherlands Cancer Institute were grown on Transwell type filters (Corning) for 4 days to confluence in DMEM/F12 media containing 10% fetal bovine serum and antibiotics as has been described previously.[43] Compounds were added to the apical side at a concentration of 10 μM in a transport buffer comprising of Hank's balanced salt solution, 25 mM D-glucose and buffered with HEPES to pH 7.4. Samples were incubated for 1 h at 37 °C and carefully collected from both the apical and basal side of the filters. Compounds selected for MDCK-mdr1 cell assays were infused on an Applied Biosystems API-4000 mass spectrometer to optimize for analysis using multiple reaction monitoring (MRM). Flow injection analysis was also conducted to optimize for mass spectrometer parameters. Samples from the apical and basolateral side of the MDCK cell assay were dried under nitrogen on a Turbovap LV. The chromatography was conducted with an Agilent 1100 binary pump with a flow rate of 0.5 mL/min. Mobile phase solvents were A, 0.1% formic acid in water, and B, 0.1% formic acid in methanol. The initial solvent conditions were 10% B for 1 min, then a gradient was used by increasing to 95% B over 5 min, then returning to initial conditions. Data reported are average values from 2 to 3 measurements.

Plasma Stability Assay. Compounds were incubated at 10 μM in rat plasma at 37 °C. A solution of each compound was prepared in ethanol at a concentration of 1 mM. A 2.5 μL volume of the 1 mM solution was added to 247.5 μL of rat plasma (adult male Sprague−Dawley) in a glass test tube in a 37 °C water bath. Samples (50 μL) were removed at 0, 30, and 60 min and immediately extracted with 3 volumes (150 μL) of methanol. Samples were centrifuged (2500 rpm for 10 min at 4 °C) to pellet protein and supernatants transferred to LC/MS vials for analysis. Samples were stored at −80 °C prior to analysis.

S9 Fraction Stability Assay. Compounds were incubated at 10 μM in rat (male Sprague−Dawley) liver S9 fraction at 37 °C. Each compound was prepared in ethanol at a concentration of 1 mM. An assay mixture containing S9 (1 mg protein/mL final concentration) and an NADPH regenerating system (NADP [1 mM final], glucose 6-phosphate [5 mM final], and glucose 6-phosphate dehydrogenase [1 U/mL final]) in a buffer consisting of 50 mM KPO_4 phosphate buffer, pH 7.4, with 3 mM $MgCl_2$ was prepared and preincubated at 37 °C for 5 min. A 10 μL volume of the 1 mM solution was added to 990 μL of assay mixture in a glass test tube at 37 °C to initiate the assay. Samples (50 μL) were removed at 0, 15, 30, 60, and 120 min and immediately extracted with 3 volumes (150 μL) of methanol, centrifuged to pellet protein, and supernatants transferred to LC/MS vials for analysis.

Animals. The Institutional Animal Care and Use Committee approved all animal experiments. Sprague−Dawley male rats (Harlan Laboratories) weighing 200−220 g at arrival were maintained on a 12 h light/dark cycle with free access to food and water at the UCLA Division of Laboratory of Animal Medicine facilities.

Behavioral Testing. Naïve rats were tested for CNS side effects before and after drug administration in the "tetrad" of tests that are classically predictive of cannabinoid receptor activation.[24] Rats were also tested for behavioral responses to tactile stimuli before and after sciatic nerve entrapment neuropathy induction. The methods for generation of this model were exactly as previously described.[44] Analgesic effectiveness of PRCBs was tested at 3-day intervals beginning 8 days after SNE surgery. Each behavioral test is described briefly below.

DOI: 10.1021/acs.jmedchem.6b00516
J. Med. Chem. 2016, 59, 7525−7543

Rotarod. Rats were tested for motor function and the ataxic effects of drugs as described previously.[4b,45] Rats were trained 72 h before the test (3 sessions 24 h apart) to remain for at least 180 s on a rotarod revolving at an acceleration of 4−40 revs over 5 min). Rats were tested 1 h before vehicle or drug injections and tested again at 2, 6, 24, and 48 h after drug or vehicle administration. The time for which the rats are able to remain on the rotarod was recorded up to a cutoff of 3 min.

Hypothermia. Rats were acclimated to a plastic restrainer apparatus (Model RTV-180 Braintree Scientific Inc.) on the day of testing by placing them in the restrainer twice for 5 min separated by 20 min. Baseline core temperature was taken before treatment, and again at 2, 6, and 24 and 48 h after drug/vehicle injection.

Catalepsy (Ring) Test. Catalepsy was determined with a ring immobility test,[46] modified for rats.[4b,24a] Rats were placed with their forepaws on a horizontal metal ring (12 cm diameter) at a height that allowed their hindpaws to just touch the bench surface. Immobility was recorded as the time for the rat to move off the ring with a 100 s cutoff. Rats were tested before vehicle/drug injections and again at 2, 6, 24, and 48 h after injection.

Tail-Flick Test. A modified Hargreaves apparatus (model 390, IITC Instr.) was also used to measure tail-flick latency (TFL). Radiant heat was directed to a point 3 cm from the tail tip and the TFL observed and timed with a photo cell counter. The intensity of the radiant heat was adjusted for a baseline TFL of approximately 5−7 s for naïve rats, with a 25 s cutoff set to avoid tissue damage.

Mechanical Sensitivity. Rats were placed in a plastic-walled cage (10 × 20 × 13 cm^3) with a metal mesh floor (0.6 × 0.6 cm^2 holes) and allowed to acclimate for 10 min. The amount of pressure (g) needed to evoke a hindpaw withdrawal response was measured 4 times on each paw separated by 30-s intervals using a von Frey-type digital meter (model 1601C, IITC Instr.). Results of 4 tests/session were averaged for each paw.

Drug Administration. For intraperitoneal (ip) injection, drugs were first dissolved in a 50/50% mixture of pure DMSO and Cremophor EL (Sigma-Aldrich), then appropriately diluted in sterile saline (1.5 mL/kg for ip) and administered using 271/2 gauge sterile needles and 1 cm^3 syringes equipped with a 0.22 μm filter. For oral administration, drugs were dissolved in pure DMSO, appropriately diluted in 20% sweet condensed milk (16 mL/kg), and delivered directly in the stomach by oral intubation with the aid of a ball-tipped gavage needle and a 5 cc syringe.

Body Fluid and Tissue Collection for Pharmacokinetics Assays. (A) Plasma collection: rats were administered CB1R ligands and blood samples (~110 μL) collected from the tail vein at various intervals after brief (<5 min) placement in a plastic restraining apparatus (RTV-180, Braintree Scientific Inc., Braintree, MA). Samples were centrifuged at 12000 rpm for 3 min and the plasma supernatant (~50 μL) placed in heparinized capillary tubes and stored at −20 °C until analysis. (B) CSF collection: rats were anesthetized (isoflurane) placed in a stereotactic frame, the dura exposed at the level of the cisterna magna, 100−150 μL of CSF collected as per,[47] and stored at −20 °C until analysis. (C) Brain collection: rats were terminally anesthetized (pentobarbital, 75 mg/kg), perfused intracardially with 60 mL of cold saline, and the brain rapidly removed and stored at −20 °C until analysis.

Mass Spectroscopy Analysis of Fluid and Tissue Samples. Plasma, CSF, and brain samples were analyzed by LC-MS/MS and quantified using standard curves prepared from appropriate drug dilutions in samples obtained from untreated animals.[48]

Statistical Analysis. The investigator performing all of the behavioral tests was blind to the dose and nature of drugs administered to the rats. One-way or two-way repeated measurements analysis of variance (RM ANOVA) were used to assess significance of drug effects.

■ ASSOCIATED CONTENT

Supporting Information

The Supporting Information is available free of charge on the ACS Publications website at DOI: 10.1021/acs.jmedchem.6b00516.

Molecular formula strings (CSV)

■ AUTHOR INFORMATION

Corresponding Authors

*For H.H.S.: phone, 919-541-6690; E-mail, hhs@rti.org.

*For I.S.: phone, 310-825-3190; fax, 310-794-7109; E-mail, igor@ucla.edu.

Notes

The authors declare no competing financial interest.

■ ACKNOWLEDGMENTS

We thank Bradley Snyder, Andrei Marechek, Dmitry Ivanov, and Daniel Malkin for help with behavioral studies at UCLA. This work was made possible with support by NIH grant DA023163 (I.S., H.H.S.), UCLA Academic Senate Faculty Grant (I.S.), and UCLA Graduate Studies stipend (Y.M.).

■ ABBREVIATIONS USED

BBB, blood−brain barrier; BNB, blood−nerve barrier; CB, cannabinoid; CB1R, cannabinoid 1 receptor; CB2R, cannabinoid 2 receptor; CNS, central nervous system; CSF, cerebrospinal fluid; ECBs, endocannabinoids; MDCK, Madin−Darby canine kidney; PRCBs, peripherally restricted cannabinoids; SNE, sciatic nerve entrapment; TFL, tail-flick latency

■ REFERENCES

(1) (a) Johannes, C. B.; Le, T. K.; Zhou, X.; Johnston, J. A.; Dworkin, R. H. The prevalence of chronic pain in United States adults: results of an Internet-based survey. *J. Pain* **2010**, *11*, 1230−1239. (b) Sessle, B. Unrelieved pain: a crisis. *Pain Res. Manag.* **2011**, *16*, 416−420.

(2) (a) Ossipov, M. H.; Porreca, F. Challenges in the development of novel treatment strategies for neuropathic pain. *NeuroRx* **2005**, *2*, 650−661. (b) Kinloch, R. A.; Cox, P. J. New targets for neuropathic pain therapeutics. *Expert Opin. Ther. Targets* **2005**, *9*, 685−698. (c) Sullivan, M. D.; Howe, C. Q. Opioid therapy for chronic pain in the United States: promises and perils. *Pain* **2013**, *154* (Suppl1), S94−S100.

(3) (a) Karst, M.; Salim, K.; Burstein, S.; Conrad, I.; Hoy, L.; Schneider, U. Analgesic effect of the synthetic cannabinoid CT-3 on chronic neuropathic pain: a randomized controlled trial. *JAMA* **2003**, *290*, 1757−1762. (b) Berman, J. S.; Symonds, C.; Birch, R. Efficacy of two cannabis based medicinal extracts for relief of central neuropathic pain from brachial plexus avulsion: results of a randomised controlled trial. *Pain* **2004**, *112*, 299−306. (c) Notcutt, W.; Price, M.; Miller, R.; Newport, S.; Phillips, C.; Simmons, S.; Sansom, C. Initial experiences with medicinal extracts of cannabis for chronic pain: results from 34 'N of 1' studies. *Anaesthesia* **2004**, *59*, 440−452.

(4) (a) Herzberg, U.; Eliav, E.; Bennett, G. J.; Kopin, I. J. The analgesic effects of R(+)-WIN 55,212−2 mesylate, a high affinity cannabinoid agonist, in a rat model of neuropathic pain. *Neurosci. Lett.* **1997**, *221*, 157−160. (b) Fox, A.; Kesingland, A.; Gentry, C.; McNair, K.; Patel, S.; Urban, L.; James, I. The role of central and peripheral Cannabinoid$_1$ receptors in the antihyperalgesic activity of cannabinoids in a model of neuropathic pain. *Pain* **2001**, *92*, 91−100.

(5) Mackie, K. Distribution of cannabinoid receptors in the central and peripheral nervous system. *Handb. Exp. Pharmacol.* **2005**, *168*, 299−325.

(6) (a) Amaya, F.; Shimosato, G.; Kawasaki, Y.; Hashimoto, S.; Tanaka, Y.; Ji, R. R.; Tanaka, M. Induction of CB1 cannabinoid receptor by inflammation in primary afferent neurons facilitates antihyperalgesic effect of peripheral CB1 agonist. *Pain* **2006**, *124*, 175−183. (b) Gutierrez, T.; Farthing, J. N.; Zvonok, A. M.; Makriyannis, A.; Hohmann, A. G. Activation of peripheral cannabinoid CB1 and CB2 receptors suppresses the maintenance of inflammatory nociception: a comparative analysis. *Br. J. Pharmacol.* **2007**, *150*, 153−163. (c) Johanek, L. M.; Simone, D. A. Activation of peripheral cannabinoid receptors attenuates cutaneous hyperalgesia produced by a heat injury. *Pain* **2004**, *109*, 432−442. (d) Richardson, J. D.; Kilo, S.; Hargreaves, K. M.

DOI: 10.1021/acs.jmedchem.6b00516
J. Med. Chem. 2016, 59, 7525−7543

Cannabinoids reduce hyperalgesia and inflammation via interaction with peripheral CB1 receptors. *Pain* **1998**, *75*, 111−119.
(7) Agarwal, N.; Pacher, P.; Tegeder, I.; Amaya, F.; Constantin, C. E.; Brenner, G. J.; Rubino, T.; Michalski, C. W.; Marsicano, G.; Monory, K.; Mackie, K.; Marian, C.; Batkai, S.; Parolaro, D.; Fischer, M. J.; Reeh, P.; Kunos, G.; Kress, M.; Lutz, B.; Woolf, C. J.; Kuner, R. Cannabinoids mediate analgesia largely via peripheral type 1 cannabinoid receptors in nociceptors. *Nat. Neurosci.* **2007**, *10*, 870−879.
(8) Spigelman, I. Frontiers in neuroscience: therapeutic targeting of peripheral cannabinoid receptors in inflammatory and neuropathic pain states. In *Translational Pain Research: from Mouse to Man*; Kruger, L., Light, A. R., Eds.; Taylor & Francis Group, LLC: Boca Raton, FL, 2010; pp 99−137.
(9) Pertwee, R. G. The diverse CB1 and CB2 receptor pharmacology of three plant cannabinoids: Δ9-tetrahydrocannabinol, cannabidiol and Δ9-tetrahydrocannabivarin. *Br. J. Pharmacol.* **2008**, *153*, 199−215.
(10) (a) Bridges, D.; Ahmad, K.; Rice, A. S. The synthetic cannabinoid WIN55,212−2 attenuates hyperalgesia and allodynia in a rat model of neuropathic pain. *Br. J. Pharmacol.* **2001**, *133*, 586−594. (b) Costa, B.; Colleoni, M.; Conti, S.; Trovato, A. E.; Bianchi, M.; Sotgiu, M. L.; Giagnoni, G. Repeated treatment with the synthetic cannabinoid WIN 55,212−2 reduces both hyperalgesia and production of pronociceptive mediators in a rat model of neuropathic pain. *Br. J. Pharmacol.* **2004**, *141*, 4−8.
(11) (a) Mao, J.; Price, D. D.; Mayer, D. J. Experimental mononeuropathy reduces the antinociceptive effects of morphine: implications for common intracellular mechanisms involved in morphine tolerance and neuropathic pain. *Pain* **1995**, *61*, 353−364. (b) Ossipov, M. H.; Lopez, Y.; Nichols, M. L.; Bian, D.; Porreca, F. The loss of antinociceptive efficacy of spinal morphine in rats with nerve ligation injury is prevented by reducing spinal afferent drive. *Neurosci. Lett.* **1995**, *199*, 87−90. (c) Rashid, M. H.; Inoue, M.; Toda, K.; Ueda, H. Loss of peripheral morphine analgesia contributes to the reduced effectiveness of systemic morphine in neuropathic pain. *J. Pharmacol. Exp. Ther.* **2004**, *309*, 380−387. (d) Ballantyne, J. C. Opioid analgesia: perspectives on right use and utility. *Pain Physician* **2007**, *10*, 479−491. (e) Ballantyne, J. C.; LaForge, K. S. Opioid dependence and addiction during opioid treatment of chronic pain. *Pain* **2007**, *129*, 235−255. (f) Holtman, J. R., Jr.; Jellish, W. S. Opioid-induced hyperalgesia and burn pain. *J. Burn Care Res.* **2012**, *33*, 692−701. (g) Pohl, M.; Smith, L. Chronic pain and addiction: challenging co-occurring disorders. *J. Psychoact. Drugs* **2012**, *44*, 119−124.
(12) (a) Calignano, A.; La Rana, G.; Giuffrida, A.; Piomelli, D. Control of pain initiation by endogenous cannabinoids. *Nature* **1998**, *394*, 277−281. (b) Elmes, S. J.; Winyard, L. A.; Medhurst, S. J.; Clayton, N. M.; Wilson, A. W.; Kendall, D. A.; Chapman, V. Activation of CB_1 and CB_2 receptors attenuates the induction and maintenance of inflammatory pain in the rat. *Pain* **2005**, *118*, 327−335. (c) Malan, T. P., Jr.; Ibrahim, M. M.; Deng, H.; Liu, Q.; Mata, H. P.; Vanderah, T.; Porreca, F.; Makriyannis, A. CB_2 cannabinoid receptor-mediated peripheral antinociception. *Pain* **2001**, *93*, 239−245. (d) Nackley, A. G.; Suplita, R. L.; Hohmann, A. G. A peripheral cannabinoid mechanism suppresses spinal fos protein expression and pain behavior in a rat model of inflammation. *Neuroscience* **2003**, *117*, 659−670. (e) Quartilho, A.; Mata, H. P.; Ibrahim, M. M.; Vanderah, T. W.; Porreca, F.; Makriyannis, A.; Malan, T. P., Jr. Inhibition of inflammatory hyperalgesia by activation of peripheral CB2 cannabinoid receptors. *Anesthesiology* **2003**, *99*, 955−960. (f) Guindon, J.; Beaulieu, P. Antihyperalgesic effects of local injections of anandamide, ibuprofen, rofecoxib and their combinations in a model of neuropathic pain. *Neuropharmacology* **2006**, *50*, 814−823.
(13) (a) Cheng, Y. X.; Pourashraf, M.; Luo, X.; Srivastava, S.; Walpole, C.; Salois, D.; St-Onge, S.; Payza, K.; Lessard, E.; Yu, X. H.; Tomaszewski, M. J. γ-Carbolines: a novel class of cannabinoid agonists with high aqueous solubility and restricted CNS penetration. *Bioorg. Med. Chem. Lett.* **2012**, *22*, 1619−1624. (b) Dziadulewicz, E. K.; Bevan, S. J.; Brain, C. T.; Coote, P. R.; Culshaw, A. J.; Davis, A. J.; Edwards, L. J.; Fisher, A. J.; Fox, A. J.; Gentry, C.; Groarke, A.; Hart, T. W.; Huber, W.; James, I. F.; Kesingland, A.; La Vecchia, L.; Loong, Y.; Lyothier, I.; McNair, K.; O'Farrell, C.; Peacock, M.; Portmann, R.; Schopfer, U.; Yaqoob, M.; Zadrobilek, J. Naphthalen-1-yl-(4-pentyloxynaphthalen-1-yl)methanone: a potent, orally bioavailable human CB1/CB2 dual agonist with antihyperalgesic properties and restricted central nervous system penetration. *J. Med. Chem.* **2007**, *50*, 3851−3856. (c) Yu, X. H.; Cao, C. Q.; Martino, G.; Puma, C.; Morinville, A.; St-Onge, S.; Lessard, E.; Perkins, M. N.; Laird, J. M. A peripherally restricted cannabinoid receptor agonist produces robust anti-nociceptive effects in rodent models of inflammatory and neuropathic pain. *Pain* **2010**, *151*, 337−344. (d) Clapper, J. R.; Moreno-Sanz, G.; Russo, R.; Guijarro, A.; Vacondio, F.; Duranti, A.; Tontini, A.; Sanchini, S.; Sciolino, N. R.; Spradley, J. M.; Hohmann, A. G.; Calignano, A.; Mor, M.; Tarzia, G.; Piomelli, D. Anandamide suppresses pain initiation through a peripheral endocannabinoid mechanism. *Nat. Neurosci.* **2010**, *13*, 1265−1270.
(14) Hind, W. H.; Tufarelli, C.; Neophytou, M.; Anderson, S. I.; England, T. J.; O'Sullivan, S. E. Endocannabinoids modulate human blood-brain barrier permeability in vitro. *Br. J. Pharmacol.* **2015**, *172*, 3015−3027.
(15) (a) Huffman, J. W.; Mabon, R.; Wu, M. J.; Lu, J.; Hart, R.; Hurst, D. P.; Reggio, P. H.; Wiley, J. L.; Martin, B. R. 3-Indolyl-1-naphthylmethanes: new cannabimimetic indoles provide evidence for aromatic stacking interactions with the CB_1 cannabinoid receptor. *Bioorg. Med. Chem.* **2003**, *11*, 539−549. (b) Carroll, F. I.; Lewin, A. H.; Mascarella, S. W.; Seltzman, H. H.; Reddy, P. A. Designer drugs: a medicinal chemistry perspective. *Ann. N. Y. Acad. Sci.* **2012**, *1248*, 18−38. (c) Huffman, J. W.; Zengin, G.; Wu, M. J.; Lu, J.; Hynd, G.; Bushell, K.; Thompson, A. L.; Bushell, S.; Tartal, C.; Hurst, D. P.; Reggio, P. H.; Selley, D. E.; Cassidy, M. P.; Wiley, J. L.; Martin, B. R. Structure-activity relationships for 1-alkyl-3-(1-naphthoyl)indoles at the cannabinoid CB(1) and CB(2) receptors: steric and electronic effects of naphthoyl substituents. New highly selective CB(2) receptor agonists. *Bioorg. Med. Chem.* **2005**, *13*, 89−112.
(16) Innocenzi, P.; Benchikh, E.; Fitzgerald, P.; Lowry, P.; McConnell, I. Detection of synthetic cannabinoids. EP2487155A1, 2012.
(17) Reggio, P. H.; Basu-Dutt, S.; Barnett-Norris, J.; Castro, M. T.; Hurst, D. P.; Seltzman, H. H.; Roche, M. J.; Gilliam, A. F.; Thomas, B. F.; Stevenson, L. A.; Pertwee, R. G.; Abood, M. E. The bioactive conformation of aminoalkylindoles at the cannabinoid CB1 and CB2 receptors: insights gained from (E)- and (Z)-naphthylidene indenes. *J. Med. Chem.* **1998**, *41*, 5177−5187.
(18) Mosconi, T.; Kruger, L. Fixed-diameter polyethylene cuffs applied to the rat sciatic nerve induce a painful neuropathy: Ultrastructural morphometric analysis of axonal alterations. *Pain* **1996**, *64*, 37−57.
(19) Pitcher, G. M.; Ritchie, J.; Henry, J. L. Nerve constriction in the rat: model of neuropathic, surgical and central pain. *Pain* **1999**, *83*, 37−46.
(20) Bailey, A. L.; Ribeiro-da-Silva, A. Transient loss of terminals from non-peptidergic nociceptive fibers in the substantia gelatinosa of spinal cord following chronic constriction injury of the sciatic nerve. *Neuroscience* **2006**, *138*, 675−690.
(21) (a) Thakor, D. K.; Lin, A.; Matsuka, Y.; Meyer, E. M.; Ruangsri, S.; Nishimura, I.; Spigelman, I. Increased peripheral nerve excitability and local NaV1.8 mRNA up-regulation in painful neuropathy. *Mol. Pain* **2009**, *5*, 14. (b) Ruangsri, S.; Lin, A.; Mulpuri, Y.; Lee, K.; Spigelman, I.; Nishimura, I. Relationship of axonal voltage-gated sodium channel 1.8 (NaV1.8) mRNA accumulation to sciatic nerve injury-induced painful neuropathy in rats. *J. Biol. Chem.* **2011**, *286*, 39836−39847.
(22) Martin, I. Prediction of blood-brain barrier penetration: are we missing the point? *Drug Discovery Today* **2004**, *9*, 161−162.
(23) Adam, J. M.; Clark, J. K.; Davies, K.; Everett, K.; Fields, R.; Francis, S.; Jeremiah, F.; Kiyoi, T.; Maidment, M.; Morrison, A.; Ratcliffe, P.; Prosser, A.; Schulz, J.; Wishart, G.; Baker, J.; Boyce, S.; Campbell, R.; Cottney, J. E.; Deehan, M.; Martin, I. Low brain penetrant CB1 receptor agonists for the treatment of neuropathic pain. *Bioorg. Med. Chem. Lett.* **2012**, *22*, 2932−2937.
(24) (a) Martin, B. R.; Compton, D. R.; Thomas, B. F.; Prescott, W. R.; Little, P. J.; Razdan, R. K.; Johnson, M. R.; Melvin, L. S.; Mechoulam, R.; Ward, S. J. Behavioral, biochemical, and molecular modeling evaluations of cannabinoid analogs. *Pharmacol., Biochem. Behav.* **1991**, *40*, 471−478. (b) Smith, P. B.; Compton, D. R.; Welch, S. P.; Razdan, R. K.;

DOI: 10.1021/acs.jmedchem.6b00516
J. Med. Chem. 2016, 59, 7525−7543

Mechoulam, R.; Martin, B. R. The pharmacological activity of anandamide, a putative endogenous cannabinoid, in mice. *J. Pharmacol. Exp. Ther.* **1994**, *270*, 219−227. (c) Compton, D. R.; Rice, K. C.; de Costa, B. R.; Razdan, R. K.; Melvin, L. S.; Johnson, M. R.; Martin, B. R. Cannabinoid structure−activity relationships: correlation of receptor binding and in vivo activities. *J. Pharmacol. Exp. Ther.* **1993**, *265*, 218−226.

(25) Devane, W. A.; Breuer, A.; Sheskin, T.; Jarbe, T. U.; Eisen, M. S.; Mechoulam, R. A novel probe for the cannabinoid receptor. *J. Med. Chem.* **1992**, *35*, 2065−2069.

(26) Rinaldi-Carmona, M.; Barth, F.; Heaulme, M.; Shire, D.; Calandra, B.; Congy, C.; Martinez, S.; Maruani, J.; Neliat, G.; Caput, D.; Ferrara, P.; Soubrié, P.; Brelière, J. C.; Le Fur, G. SR141716A, a potent and selective antagonist of the brain cannabinoid receptor. *FEBS Lett.* **1994**, *350*, 240−244.

(27) Fulp, A.; Bortoff, K.; Seltzman, H.; Zhang, Y.; Mathews, J.; Snyder, R.; Fennell, T.; Maitra, R. Design and synthesis of cannabinoid receptor 1 antagonists for peripheral selectivity. *J. Med. Chem.* **2012**, *55*, 2820−2834.

(28) D'Ambra, T. E.; Estep, K. G.; Bell, M. R.; Eissenstat, M. A.; Josef, K. A.; Ward, S. J.; Haycock, D. A.; Baizman, E. R.; Casiano, F. M.; Beglin, N. C.; Chippari, S. M.; Grego, J. D.; Kullnig, R. K.; Daley, G. T. Conformationally restrained analogues of pravadoline: nanomolar potent, enantioselective, (aminoalkyl)indole agonists of the cannabinoid receptor. *J. Med. Chem.* **1992**, *35*, 124−135.

(29) Wang, Q.; Rager, J. D.; Weinstein, K.; Kardos, P. S.; Dobson, G. L.; Li, J.; Hidalgo, I. J. Evaluation of the MDR-MDCK cell line as a permeability screen for the blood-brain barrier. *Int. J. Pharm. (Amsterdam, Neth.)* **2005**, *288*, 349−359.

(30) (a) McAllister, S. D.; Rizvi, G.; Anavi-Goffer, S.; Hurst, D. P.; Barnett-Norris, J.; Lynch, D. L.; Reggio, P. H.; Abood, M. E. An aromatic microdomain at the cannabinoid CB_1 receptor constitutes an agonist/inverse agonist binding region. *J. Med. Chem.* **2003**, *46*, 5139−5152. (b) Reggio, P. H. Pharmacophores for ligand recognition and activation/inactivation of the cannabinoid receptors. *Curr. Pharm. Des.* **2003**, *9*, 1607−1633.

(31) Eissenstat, M. A.; Bell, M. R.; D'Ambra, T. E.; Alexander, E. J.; Daum, S. J.; Ackerman, J. H.; Gruett, M. D.; Kumar, V.; Estep, K. G.; Olefirowicz, E. M.; Wetzel, J. R.; Alexander, M. D.; Weaver, J. D., III; Haycock, D. A.; Luttinger, D. A.; Casiano, F. M.; Chippari, S. M.; Kuster, J. E.; Stevenson, J. I.; Ward, S. J. Aminoalkylindoles: structure-activity relationships of novel cannabinoid mimetics. *J. Med. Chem.* **1995**, *38*, 3094−3105.

(32) Huffman, J. W.; Szklennik, P. V.; Almond, A.; Bushell, K.; Selley, D. E.; He, H.; Cassidy, M. P.; Wiley, J. L.; Martin, B. R. 1-Pentyl-3-phenylacetylindoles, a new class of cannabimimetic indoles. *Bioorg. Med. Chem. Lett.* **2005**, *15*, 4110−4113.

(33) (a) Brents, L. K.; Gallus-Zawada, A.; Radominska-Pandya, A.; Vasiljevik, T.; Prisinzano, T. E.; Fantegrossi, W. E.; Moran, J. H.; Prather, P. L. Monohydroxylated metabolites of the K2 synthetic cannabinoid JWH-073 retain intermediate to high cannabinoid 1 receptor (CB1R) affinity and exhibit neutral antagonist to partial agonist activity. *Biochem. Pharmacol. (Amsterdam, Neth.)* **2012**, *83*, 952−961. (b) Brents, L. K.; Reichard, E. E.; Zimmerman, S. M.; Moran, J. H.; Fantegrossi, W. E.; Prather, P. L. Phase I hydroxylated metabolites of the K2 synthetic cannabinoid JWH-018 retain in vitro and in vivo cannabinoid 1 receptor affinity and activity. *PLoS One* **2011**, *6*, e21917.

(34) Löscher, W.; Potschka, H. Role of drug efflux transporters in the brain for drug disposition and treatment of brain diseases. *Prog. Neurobiol.* **2005**, *76*, 22−76.

(35) Montesinos, R. N.; Moulari, B.; Gromand, J.; Beduneau, A.; Lamprecht, A.; Pellequer, Y. Coadministration of P-glycoprotein modulators on loperamide pharmacokinetics and brain distribution. *Drug Metab. Dispos.* **2014**, *42*, 700−706.

(36) Fuchs, H.; Kishimoto, W.; Gansser, D.; Tanswell, P.; Ishiguro, N. Brain penetration of WEB 2086 (Apafant) and dantrolene in Mdr1a (P-glycoprotein) and Bcrp knockout rats. *Drug Metab. Dispos.* **2014**, *42*, 1761−1765.

(37) (a) Mitrirattanakul, S.; Ramakul, N.; Guerrero, A. V.; Matsuka, Y.; Ono, T.; Iwase, H.; Mackie, K.; Faull, K.; Spigelman, I. Site-specific increases in peripheral cannabinoid receptors and their endogenous ligands in a model of neuropathic pain. *Pain* **2006**, *126*, 102−114. (b) Wotherspoon, G.; Fox, A.; McIntyre, P.; Colley, S.; Bevan, S.; Winter, J. Peripheral nerve injury induces cannabinoid receptor 2 protein expression in rat sensory neurons. *Neuroscience* **2005**, *135*, 235−245.

(38) Ubogu, E. E. The molecular and biophysical characterization of the human blood-nerve barrier: current concepts. *J. Vasc. Res.* **2013**, *50*, 289−303.

(39) (a) Ragavendran, J. V.; Laferriere, A.; Xiao, W. H.; Bennett, G. J.; Padi, S. S.; Zhang, J.; Coderre, T. J. Topical combinations aimed at treating microvascular dysfunction reduce allodynia in rat models of CRPS-I and neuropathic pain. *J. Pain* **2013**, *14*, 66−78. (b) Greathouse, K. M.; Palladino, S. P.; Dong, C.; Helton, E. S.; Ubogu, E. E. Modeling leukocyte trafficking at the human blood-nerve barrier in vitro and in vivo geared towards targeted molecular therapies for peripheral neuroinflammation. *J. Neuroinflammation* **2016**, *13*, 3. (c) Kanda, T. Biology of the blood-nerve barrier and its alteration in immune mediated neuropathies. *J. Neurol., Neurosurg. Psychiatry* **2013**, *84*, 208−212. (d) Lim, T. K.; Shi, X. Q.; Martin, H. C.; Huang, H.; Luheshi, G.; Rivest, S.; Zhang, J. Blood-nerve barrier dysfunction contributes to the generation of neuropathic pain and allows targeting of injured nerves for pain relief. *Pain* **2014**, *155*, 954−967. (e) Ubogu, E. E. Inflammatory neuropathies: pathology, molecular markers and targets for specific therapeutic intervention. *Acta Neuropathol.* **2015**, *130*, 445−468.

(40) Martin, W. J.; Loo, C. M.; Basbaum, A. I. Spinal cannabinoids are anti-allodynic in rats with persistent inflammation. *Pain* **1999**, *82*, 199−205.

(41) Potenzieri, C.; Harding-Rose, C.; Simone, D. A. The cannabinoid receptor agonist, WIN 55, 212−2, attenuates tumor-evoked hyperalgesia through peripheral mechanisms. *Brain Res.* **2008**, *1215*, 69−75.

(42) Melvin, L. S.; Johnson, M. R.; Harbert, C. A.; Milne, G. M.; Weissman, A. A cannabinoid derived prototypical analgesic. *J. Med. Chem.* **1984**, *27*, 67−71.

(43) Fulp, A.; Bortoff, K.; Zhang, Y.; Seltzman, H.; Snyder, R.; Maitra, R. Towards rational design of cannabinoid receptor 1 (CB1) antagonists for peripheral selectivity. *Bioorg. Med. Chem. Lett.* **2011**, *21*, 5711−5714.

(44) Matsuka, Y.; Ono, T.; Iwase, H.; Mitrirattanakul, S.; Omoto, K. S.; Cho, T.; Lam, N. Y. Y.; Snyder, B.; Spigelman, I. Altered ATP release and metabolism in dorsal root ganglia of neuropathic rats. *Mol. Pain* **2008**, *4*, 66.

(45) (a) Dunham, N. W.; Miya, T. S. A note on a simple apparatus for detecting neurological deficit in rats and mice. *J. Am. Pharm. Assoc., Sci. Ed.* **1957**, *46*, 208−209. (b) Pryor, G. T.; Husain, S.; Larsen, F.; McKenzie, C. E.; Carr, J. D.; Braude, M. C. Interactions between Δ9-tetrahydrocannabinol and phencyclidine hydrochloride in rats. *Pharmacol., Biochem. Behav.* **1977**, *6*, 123−136.

(46) Pertwee, R. G. The ring test: a quantitative method for assessing the 'cataleptic' effect of cannabis in mice. *Br. J. Pharmacol.* **1972**, *46*, 753−763.

(47) Pegg, C. C.; He, C.; Stroink, A. R.; Kattner, K. A.; Wang, C. X. Technique for collection of cerebrospinal fluid from the cisterna magna in rat. *J. Neurosci. Methods* **2010**, *187*, 8−12.

(48) Hassler, C.; Zhang, Y.; Gilmour, B.; Graf, T.; Fennell, T.; Snyder, R.; Deschamps, J. R.; Reinscheid, R. K.; Garau, C.; Runyon, S. P. Identification of neuropeptide S antagonists: structure-activity relationship studies, X-ray crystallography, and in vivo evaluation. *ACS Chem. Neurosci.* **2014**, *5*, 731−744.

DOI: 10.1021/acs.jmedchem.6b00516
J. Med. Chem. 2016, 59, 7525−7543